University of Kentucky
UKnowledge

Theses and Dissertations--Electrical and Computer Engineering

Electrical and Computer Engineering

2012

METALLIC PATTERNING USING AN ATOMIC FORCE MICROSCOPE TIP AND LASER-INDUCED LIQUID DEPOSITION

Carlos Andrés Jarro Sanabria
University of Kentucky, carlos.jarro@uky.edu

Right click to open a feedback form in a new tab to let us know how this document benefits you.

Recommended Citation

Jarro Sanabria, Carlos Andrés, "METALLIC PATTERNING USING AN ATOMIC FORCE MICROSCOPE TIP AND LASER-INDUCED LIQUID DEPOSITION" (2012). *Theses and Dissertations--Electrical and Computer Engineering*. 6.
https://uknowledge.uky.edu/ece_etds/6

This Master's Thesis is brought to you for free and open access by the Electrical and Computer Engineering at UKnowledge. It has been accepted for inclusion in Theses and Dissertations--Electrical and Computer Engineering by an authorized administrator of UKnowledge. For more information, please contact UKnowledge@lsv.uky.edu.

STUDENT AGREEMENT:

I represent that my thesis or dissertation and abstract are my original work. Proper attribution has been given to all outside sources. I understand that I am solely responsible for obtaining any needed copyright permissions. I have obtained and attached hereto needed written permission statements(s) from the owner(s) of each third-party copyrighted matter to be included in my work, allowing electronic distribution (if such use is not permitted by the fair use doctrine).

I hereby grant to The University of Kentucky and its agents the non-exclusive license to archive and make accessible my work in whole or in part in all forms of media, now or hereafter known. I agree that the document mentioned above may be made available immediately for worldwide access unless a preapproved embargo applies.

I retain all other ownership rights to the copyright of my work. I also retain the right to use in future works (such as articles or books) all or part of my work. I understand that I am free to register the copyright to my work.

REVIEW, APPROVAL AND ACCEPTANCE

The document mentioned above has been reviewed and accepted by the student's advisor, on behalf of the advisory committee, and by the Director of Graduate Studies (DGS), on behalf of the program; we verify that this is the final, approved version of the student's dissertation including all changes required by the advisory committee. The undersigned agree to abide by the statements above.

Carlos Andrés Jarro Sanabria, Student

Dr. J. Todd Hastings, Major Professor

Dr. Zhi Chen, Director of Graduate Studies

METALLIC PATTERNING USING AN ATOMIC FORCE MICROSCOPE TIP AND LASER-INDUCED LIQUID DEPOSITION

THESIS

A thesis submitted in partial fulfillment of the requirements
for the degree of Master of Science in Electrical Engineering
in the College of Engineering at the University of Kentucky

By

Carlos Andrés Jarro Sanabria

Lexington, Kentucky

Director: Dr. J. Todd Hastings, Associate Professor of Electrical Engineering

Lexington, Kentucky

2012

Copyright © Carlos Andrés Jarro Sanabria 2012

ABSTRACT OF THESIS

METALLIC PATTERNING USING AN ATOMIC FORCE MICROSCOPE TIP AND LASER-INDUCED LIQUID DEPOSITION

The development of nanoscale patterns has a vast variety of applications going from biology to solid state devices. In this research we present a new direct patterning technique in which laser photoreduction of silver from a liquid is controlled by a scanning atomic force microscope tip. While pursuing the formation of patterns using the plasmonic field enhancement of an electromagnetic wave incident on a metallic Atomic Force Microscope (AFM) tip, our group discovered that contrary to expectations, the tip suppresses, rather than enhances, deposition on the underlying substrate, and this suppression persists in the absence of the tip. Experiments presented here exclude three potential mechanisms: purely mechanical material removal, depletion of the silver precursor, and preferential photoreduction on existing deposits. An example of a nano-scaled pattern was generated to show the possibilities of this work. These results represent a first step toward direct, negative tone, tip-based patterning of functional materials.

KEYWORDS: Nanoscale patterning, AFM Tip, Tip-based patterning, Silver Deposition, Laser-induced liquid Deposition.

Carlos Andrés Jarro Sanabria

Author

June 6th, 2012

Date

METALLIC PATTERNING USING AN ATOMIC FORCE MICROSCOPE TIP AND LASER-INDUCED LIQUID DEPOSITION

By

Carlos Andrés Jarro Sanabria

Dr. J. Todd Hastings

Director of Thesis

Dr. Zhi Chen

Director of Graduate Studies

June 6th, 2012

Date

DEDICATION

To my parents Jaime and Yolanda, my sisters Sandra and Lina, and my wife Claudia.

ACKNOWLEDGMENTS

I would like to thank my advisor and chair of my committee Dr. Todd Hastings, not only for letting me work in his research group but also for being a guide in the academic and career topics. Also I would like to thank the other committee members Dr. Janet Lumpp, Dr. Pinar Menguç, and Dr. Vijay Singh, for the time they took to correct me, instruct me, and help me in achieving this goal.

It is difficult to separate my friends from my colleagues and I want to thank them for that. To Gazi, Neha, and Eugene, for not being just academic collaborators but friends in which I could discharge frustrations and find support.

A special thanks to my parents for they have given me everything they could so I could achieve my goals in life. To my sisters who helped me in forging my character and for their support in any decision I have taken in my life.

Finally I owe deep gratitude to my wife, who without her support, her trust in me, and sweet ways of pressure, that I needed so much, I would have not been able to obtain my degree.

TABLE OF CONTENTS

LIST OF FIGURES

Chapter 1

INTRODUCTION

Most materials have different properties when their sizes are reduced to the nano-scale. The applications for nano-technology are so diverse that they can go from silver nano-spheres used in antibacterial cloth [1] to improved sensors in controlled substances detectors. Several devices nowadays require the use of these nanoscopic materials; however, the current fabrication processes to develop nano-patterns are expensive and complicated. A considerable amount of research is being done currently to find a reliable, inexpensive, and simple way to obtain patterns of nanometric size. This study analyzes a novel approach to obtain small silver patterns using a simple technique based on the use of Atomic Force Microscope (AFM) probes.

In the area of nanofabrication different techniques using tools like electron beam, ion beam, scanning probes, and extreme ultraviolet light sources have been used to successfully form nanopatterns. Most of these techniques work by using the previously mentioned tools to expose some type of photoresist and generate the patterns after developing the resist. Patterns of less than 20 nm width have been achieved [2].

The already nanometric size of the probes used in the scanning probe tools, has given rise to a different type of fabrication. Instead of exposing resist, the sharp probe has been used by itself to form nanopatterns. These small tips have been successfully used previously to indent surfaces [3], manipulate particles [4], and deposit particles [5]. All of these techniques have been explored further and interesting results and patterns have been obtained. However, very few people have used enhanced electric fields to deposit and pattern metals on a dielectric substrate.

This document will treat the patterning and deposition of silver on glass substrates by means of photoreduction of silver nanoparticles from liquid precursors aided by a scanning probe. We explain the experiments conducted to understand the pattern formation process

and its limitations. Conclusions and suggested future work are proposed for the improvement of this technique. As it will be shown, the new proposed methodology can be used to form negative toned patterns of less than 1 μm width. Given an enhancement in the deposits characteristics, and a variety in the materials deposited, this technique could provide a solution to a common problem identified in the industry of integrated circuit mask repair.

In the following chapter (chapter 2) a brief introduction to the equipment, technique, and theories used during this study is given. Chapter 3 will provide an overview of the research that has been done so far in the laser induced and tip aided nanofabrication. Chapter 4 will provide a description of the laser sources, liquid precursors, and AFM used in this study. Chapter 5 discusses the results and provides an explanation for the observed effects. Chapter 6 contains the conclusions reached during the development of this project and chapter 7 will present the future work needed to correct some problems detected and to improve the overall conditions of the experiments to obtain better results.

Chapter 2

EQUIPMENT, TECHNIQUES AND THEORIES IN NANO-FABRICATION

The basic tool used in this study is the atomic force microscope. With it we try to take advantage of the electric field enhancement due to a plasmonic physical effect. Hence the necessity of providing a basic explanation of the tools and theories that made possible and provided the motivation for our study.

2.1 Atomic Force Microscope Basic Operation

The scanning probe microscope (SPM) is a generic name for an instrument that acquires data from a sample while moving across a region in a sweeping mode (line by line) and at a very close distance or even in contact with the surface. SPM uses a single tip, attached to a piezoelectric device, to perform different measurements on the sample such as topography, conductivity, magnetic properties, and more. Two very popular derivations of the SPM are the scanning tunneling microscopy (STM), which is the origin of every SPM variation, and the atomic force microscopy (AFM), which is the tool used in this study. The STM uses a conductive tip to run a current across the tip and the region being scanned. The tip sample separation can be controlled precisely such that the current is kept constant as the tip scans. In contrast, the atomic force microscope uses a laser to measure the position of the tip, and does not require a conductive tip. The tip with an apex radius of usually less than 30nm is placed on the piezoelectric device which is capable of moving precisely in the sub micrometric range. The laser beam is aimed at the back of the tip and reflected to a photodetector. Figure 2.1 shows a diagram explaining the AFM components. This same setup is used for the scanning tunneling microscope (STM). The AFM has two basic modes to work: the contact mode, and the tapping mode.

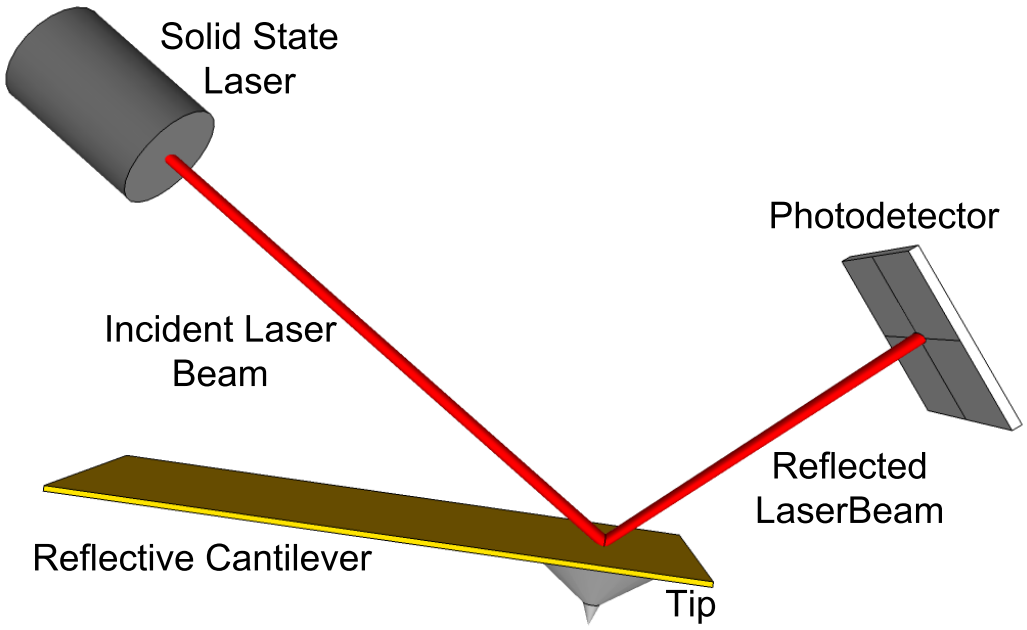

Figure 2.1: AFM basic operation diagram. The laser signal is reflected from a coated surface on the cantilever, the photodetector can sense the position of the reflected beam in four quadrants.

2.1.1 Contact Mode

In contact mode the tip is brought down until it is in contact with the surface of the sample to be read. The piezoelectric device is able to move the tip in three dimensions: X and Y, the horizontal and vertical movement on the sample's surface plane, and Z, the up/down movement in charge of approaching or withdrawing the tip from the sample. After the tip reaches the sample, the piezoelectric device moves further in the Z axis to reach a set point. This set point tells the system the force that one wants the tip to apply on the sample. Once the force set point is reached, the piezoelectric is in charge of keeping this force value constant; to achieve this it uses a proportional-integral control system which can be set depending on the sample and the reading speed conditions. The piezoelectric makes the scan by moving horizontally and vertically in the surface plane according to the scan configuration. The Z movement of the piezoelectric and the vertical position change in the laser reflection are added to give the topography values. Another value given in this mode is the friction which is obtained from the horizontal movement of the reflected laser

beam. The friction gives an idea of the lateral force the sample made when opposing to the sweeping movement of the tip.

2.1.2 Tapping Mode

The operational method of tapping mode is more complicated than the one contact mode utilizes. However, the advantage of tapping mode is that the tip does not have to be in contact with the surface of the sample. This operation mode is convenient when a soft sample needs to be imaged or the tip needs to be protected from wear. It could also provide a better resolution due to the elimination of a water meniscus present between the tip and the sample when using contact mode. In this mode the system finds a resonant frequency of the cantilever holding the tip. A different piezoelectric device, closer to the cantilever, is in charge now of continuously driving the cantilever oscillation at this resonant frequency. The photodetector now reads the amplitude of the cantilever's oscillation. When the tip approaches the surface, the amplitude of the cantilever's oscillation changes due to different forces the sample exerts on the tip. According to how close one wants the tip to the sample an amplitude set point is given. When the amplitude of the oscillation of the cantilever reaches the desired value the three axis movement piezoelectric stops approaching and the control system is in charge of keeping this amplitude constant. The topography value is now given by the small change in amplitude and the movement the piezoelectric device makes. A phase difference value comparing the driving oscillation and the oscillation of the cantilever is available to read now. The new value indicates how strongly the forces of the surface affecting the tip are. If the amplitude set point given is such that the tip gets in contact with the sample in each oscillation then the phase value is an indicator of the stickiness of the surface.

2.2 Plasmonics Theory

Plasmonic effects have been present in daily lives since centuries ago. An ancient technique uses gold and silver nanoparticles to give different colors to glass. Recently, the interest in nanophotonics has increased, and the plasmonic effects have been used and applied to state

of the art technology. Plasmonic theory studies the interaction between electromagnetic waves, specifically light, and metallic surfaces or particles. When light strikes on the interface between two materials with opposite sign in the real part of the dielectric constant, a charge density wave is generated on the interface; this is commonly referred to as surface plasmon wave or surface plasmon polariton.

2.2.1 Surface Plasmon

As mentioned before, a surface plasmon wave is formed when the interface between a metallic surface and a dielectric medium is illuminated with a wavelength at which the real part of the dielectric constants of both materials are opposite in sign. Common materials in which the real part of the dielectric constant is negative are materials in which some of the electrons behave like free electrons. Highly conductive metals like gold and silver can have this behavior. The surface plasmon wave, formed by a charge density, propagates along the metallic surface at a different wavenumber than the incident wave. However, the most important characteristic of a surface plasmon wave is the fact that light can be confined to a small region (in this case a two dimensional region), usually smaller than the wavelength of the incident light. If the metallic surface were reduced in size and became a nanoparticle the wave lacks a path to propagate, however a more interesting effect is obtained and is named localized surface plasmon (LSP).

2.2.2 Localized Surface Plasmon

If the size of the metallic surface used to generate surface plasmon waves is reduced such that there are now only metallic nanoparticles, a localized surface plasmon is generated. A localized surface plasmon is the accumulated charge density present in a material with a high number of free electrons. When light strikes a highly conductive particle of smaller size than the wavelength of the incident light the electron cloud will be excited and oscillate with the same frequency as the incident electromagnetic field but with a phase shift of 90° at resonance. This electron cloud/positively charge nuclei system is often modeled as a resonator. In fact the resonant frequency is achieved when the electrons absorb most of the energy provided by the incident wave. The fact that the particle has a size smaller than

the incident wave's wavelength, allows us to say that the energy has been confined to a size smaller than its wavelength. This phenomenon of light confinement is not only present in small nanoparticles but it can also be found in an apex of a very sharp tip.

2.3 Plasmonic Effects on Nano-particles, Substrates, and Tips

The theoretical behavior of electromagnetic fields incident on nanoparticles tips and substrates has been studied in depth during the 20th century. Nowadays, the development of faster computers and better mathematical algorithms has allowed the simulation of electromagnetic behavior in more complex geometries. The mathematical theory and the computer simulations have provided a better understanding of the enhanced electromagnetic fields and light confinement in systems based on substrates, nanoparticles and nano probes.

In 1908 Gustav Mie published a paper that solved Maxwell's equations to find the scattering of a dielectric spherical particle suspended in a homogeneous medium [6]. This solution provided the basis for analysis and simulation of field enhancement due to the illumination of a spherical nanoparticle. Mie proposed a solution in which the enhancement of the field depended on the size, wavelength, and the indices of refraction of the particle and the medium. Specifically, the field enhancement increases when the particle size decreases or when the illumination wavelength increases [7].

Clearly a plasmonic field enhancement is not only present in spherical nanoparticles. Based on simulations of electromagnetic behavior in nanoscale objects several authors have studied the effect of the plasmonic enhancement on sharp tips and sharp tips on substrates. These studies relate better to the research done by our laboratory group. The tip and tip-substrate geometry studies have returned these basic conclusions. The field enhancement is reduced as one moves farther away from the apex of the tip, the proximity of the tip to a dielectric substrate affects the shape of the enhancement, the size of the tip affects the amount the electric field gets enhanced, and the incidence angle and polarization affects the location along the tip where the field enhancement is maximum [8, 9, 10].

When the tip is in proximity of a spherical metallic nanoparticle an effect similar to the substrate-tip proximity is generated. This effect and geometry have been studied before and

simulation work has been done by different authors [10, 11]. For the tip-particle geometry the maximum field enhancement is obtained between the tip and the particle, and the intensity of the field below the tip's apex can be up to two orders of magnitude higher than the intensity of the incident field [9]. Figure 2.2, copied with permission from Huda et al. [11], shows a simulation of the electric field enhancement in a tip-nanoparticle-substrate geometry. In this case the tip (silicon), nanoparticle (gold), and substrate (glass) are being illuminated, through the glass substrate, with a 532 nm wavelength plane wave at 50° from the normal. The colors show the norm of the electric field, ranging from zero (blue) to 27.338 (red) V/m for 5 nm vertical separation

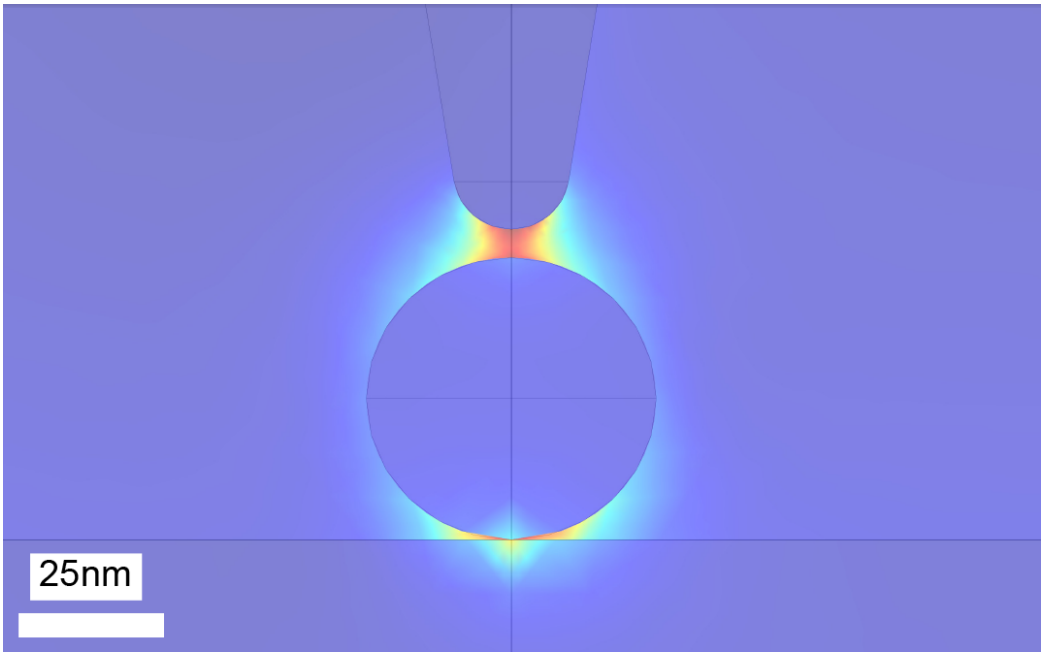

Figure 2.2: Plasmonic field enhancement on a tip-nanoparticle-substrate geometry. A glass substrate, a gold nanoparticle, and a silicon tip are illuminated with a 532nm wavelength plane wave coming at a 50° angle. The figure shows the enhanced electric field. The red color is 27 times higher than the incident wave.

Chapter 3

LITERATURE REVIEW IN TIP AIDED, AND LASER INDUCED NANO-FABRICATION

Techniques to form nano-patterns of noble metals such as gold, silver, copper, and palladium have been developed continuously and very diverse technologies are being used for fabrication [12, 13, 14, 15, 16].

3.1 Laser-induced Nano-fabrication

Several groups have also directly deposited noble metals from solution using chemical reactions triggered with a laser beam. This method is called laser-induced chemical deposition (LICD) [17, 18, 19, 20, 21]. Most of these studies use liquid precursors to deposit copper, palladium, silver, gold, and even zinc oxide. The materials this study desired to deposit are silver, gold and copper. Hence, this chapter will only review the deposition of these metals.

To deposit copper authors have used aqueous solutions based in simple salts like copper sulfate [22, 23], copper chloride [24] or larger molecules like copper acetylacetonate [25], or copper formate [18]. Kordȁ et al. [23] and Man'shina et al. [24] use a reducing agent so that the laser illumination photoreduce the copper efficiently. Except for Ouchi et al. [25] and Kim et al. [18], who use an ultraviolet light, the copper photoreduction is made with a 488 nm continuous wave argon laser. The approach used by Kim et al. [18] is much more complex; they spray copper formate in a liquid form and let it evaporate until it forms a gel like paste. Once this paste is formed, the sample is illuminated with an ultraviolet laser. Only the illuminated areas are solidified and the paste residue is washed with DI water. The minimum width of the copper patterns achieved with LICD is 3 μm.

The deposition of silver and gold on different substrates has achieved a special interest in researchers due to the application of surface enhanced Raman scattering (SERS). Several

authors have used the photoreduction of liquid precursors to elaborate Raman measurement applications [17, 13, 26]. The main solution researchers use to deposit gold by means of photoreduction contains sodium tetrachloroaurate ($NaAuCl_4$) [27, 28]. Niidome et al. use a pulsed laser in the wavelength of 532nm and sodium borohydride as a reducing agent based on Brust et al. [29]; the illumination method used by Toth et al. is a continuous wave argon laser at the 488nm wavelength and the solution contained formaldehyde as a reducing agent. Although these authors achieved a successful deposition they did not worry about generating patterns smaller than 100 μm. Most of the authors use silver nitrate in aqueous solutions to photoreduce silver onto different substrates. The illumination source varies from pulsed lasers [17, 30, 10], continuous wave lasers [31, 13, 32, 21], and even white light [33]. In terms of the illumination wavelength the frequencies go from visible (514nm) to ultraviolet (193nm). Every author deposited silver successfully on every substrate they tested. However, due to the nature of their application, the smallest feature achieved measured less than 2 μm [13].

Due to diffraction limit most of the patterns generated with just a laser beam cannot be smaller than 200 nm. Hence, another component has to be included in the method in order to generate nano-scaled patterns.

3.2 Tip Aided Nano-fabrication

In pursuit of smaller features and narrower patterns, tip aided or induced nano-fabrication was developed because of the advantage of the small dimensions of the probe, and the ease with which one can move the probe and generate almost any pattern. Tip based nano-fabrication has been divided in several areas and as technologies keep being developed more ways to categorize the methodologies will be generated [34, 35, 36, 37].

3.2.1 Material Modification

Under this category, developments have been made to use the AFM tip as a tool to drive chemical reactions or electrical modifications to preprocessed samples. A common technique used is local oxidation. In local oxidation, the probe is negatively biased with respect to

the sample and the AFM is used in contact mode or very close to the sample such that a water meniscus is formed. A semiconductor substrate is then oxidized wherever the tip is biased above a threshold voltage necessary to produce the chemical reaction [38, 39]. This technique can be applied to an etching process, because of the different etching rate of the oxide, mask fabrication, and metal oxide semiconductor (MOS) processes.

Another method of nanopatterning that could fall into this category is the exposure of a photoresist by passing a current through the tip. Some of the pioneers in using this technique were McCord and Pease [40] who in 1988 were able to achieve patterns of 22nm in width. Lee, et al. [41] used a process to expose a silane resist layer using a gold coated AFM tip. This tip is not only in charge of drawing the pattern but also its coating provides gold seeds for a future development process using a gold compound. This technique generates patterns of less than 120 nm. This technique has not been widely adopted because electron beam lithography can from much narrower patterns and is much faster than an SPM.

Under this category one could classify a local change in the electrical properties of the sample material. An electric field can be applied to a sharp tip to induce a local surface charge on a substrate. Depending on the properties of this substrate, it is not rare for charge density to remain unchanged for days if it is not externally excited [42, 43]. The AFM can be used in tapping mode to detect changes in the electric field in the sample (electrostatic force microscopy). The ability of writing and reading these charge differences is why this process can be classified as tip-based patterning.

3.2.2 Material Removal

Due to the development of stronger tips it is possible now to remove material previously deposited by applying a force on the sample with the tip and move it through the area of material one desires to remove. This technique is called AFM scratching and when related to pre-deposited self-assembled monolayers that are being removed or reorganized some researchers use the term nanoshaving [44, 45]. Given that it is possible to form very thin layers of resist, several authors have used nano-scratching as replacement of the irradiation-development steps in lithography [46, 47].

Some authors have used an STM, or a voltage biased AFM to etch material directly,

without a chemical etching, where they use the tip as a low energy electron source [48, 49]. However, most of the research in etchant aided by a SPM is for locally controlling a wet or dry chemical etching [50, 51, 52].

An interesting tool that could fall within the material removal category is thermal nanolithography. For this type of lithography the tip is heated by means of a resistive heating or a laser system in order to generate some change in the surface of the sample. The most representative example of this method was developed by Mamin [53] in 1996 to improve data storage density. Mamin designed a special tip for an AFM that was attached to a resistive heater. When the tip reached certain temperature the heat formed holes in the surface of the substrate. This development generated a research project that ended in the design of the "millipede" [54]. This device can write and read information by means of an array of resistively heated tips. The laser heated tip method will be treated below in section 3.3.

3.2.3 Material Deposition

An interesting method of material deposition uses transference of material from the tip to the substrate. Tips coated with a metal and biased with a potential can at some points deposit the coating onto the substrate being scanned. This leads to deposits of very small quantities of material and hence, very small patterns [55, 56, 57].

Another more common method used for material deposition can be named localized chemical deposition. In this approach the sample is scanned in a chemical vapor or liquid deposition environment and the tip usually biased is in charge of driving a chemical reaction so that the vaporized or liquid material can be deposited on to the substrate. Several authors have investigated this way of deposition with several material and substrate combinations [58, 59, 60].

Probably the most popular material deposition technique since it was discovered by Piner et al. [5] is dip-pen nanolithography. Its name comes from the similarity with quill or fountain pen in which one dips the pen in a container with ink, the pen absorbs the ink and then releases it when it contacts the paper. In dip-pen nanolithography an atomic force microscope in contact mode is used inside a humid environment such that a water meniscus

is formed around the apex of the tip. The probe is moved to a location where a solution of the material to be deposited or "ink" is accumulated. The ink will attach to the tip because of the water meniscus and it can be transported to the place where the pattern is desired. The material is deposited as the tip scans the surface of the substrate. Multiple material-substrate combinations have been made and the inks can go from inorganic compounds to biological specimens [61]. A derivation of dip-pen lithography is used when the tip is biased and this potential difference triggers a chemical reaction in the ink which also leads to deposition of material [62, 63].

3.2.4 Material Manipulation

Manipulation of particles [4, 64, 65], clusters of particles [66, 67], molecules [68], and even individual atoms [69, 70, 71] is possible now due to the improvements in SPM systems. Within this particles or clusters of particles one can include organic components like DNA [72, 73]. Multiple investigations have been made to model the physics of the interaction between particle and tip and several theories have been proposed [74, 4, 64]. However, the basic idea behind particle manipulation is very simple: the AFM tip is positioned where the particle is located, and then, either in contact mode or in tapping mode, the tip is moved to a location where one wants to move the particle. Nanoparticle movements have been done in vacuum, in air, and even in liquid. In the case of atomic movement the tool is more complicated. Usually these experiments are made with an STM probe. The individual atom movement has to be made usually under high vacuum to reduce unwanted contaminants and with very low temperatures to avoid diffusion of the moved atom. However, movement of silicon atoms has been made under room temperature conditions [75, 76]. Nanomanipulation has been booming nowadays due to the necessity of moving nanowires or carbon nanotubes to specific locations such that different measurements can be done on them [77, 78]. An interesting instrument created to ease the nanoparticle manipulation is the AFM nano tweezers developed by Xie et al [79]. This tool uses four piezoelectric devices: two for each of the probes and two for the stage, one for positioning and one for scanning. The AFM nano tweezers have been used successfully to overlap two gold nanowires. Since each of the

particles, clusters, or atoms has to be moved one by one, material nanomanipulation is a very slow and complicated process when trying to generate large or complex patterns.

3.3 Laser and Tip Aided Nano-fabrication

Most of the effects treated in section 3.2 (material modification, removal, deposition and manipulation), made with biased and unbiased tips, can be enhanced or accelerated by introducing an external source of energy such as laser illumination. This happens because of the enhanced electric field on the AFM tip due to charge concentration. By aiming pulsed and continuous wave lasers at the apex of the tip of an AFM or an STM, researchers have achieved thermal oxidation [80], controlled nanoscratching [81, 82], resist exposure [83], material modification [84], and chemical modification [85].

It is convenient to note that current research in scanning near-field optical microscopy (SNOM) has originated several methods to modify, remove, deposit and manipulate scanned material. Hence, a new area of nanofabrication has emerged called SNOM lithography or SNOML. The advances in this area are not going to be discussed here but they are explained in Tseng [86].

The study this thesis describes is based on AFM patterning, laser induced deposition, and liquid deposition. A liquid silver precursor, typically an aqueous solution, is illuminated with a focused laser beam to obtain deposition of solid silver on a glass substrate. While the interface of the glass slide and the liquid precursor is illuminated, an AFM tip scans the illuminated area. According to plasmonic theory principles, the incidence of light on a metallic sharp tip surrounded by a media with a different permittivity generates a charge accumulation at the surface of the tip. If the deposition due to the irradiation of the liquid precursor depends in some degree on the intensity of the illumination, a higher light intensity could accelerate the photoreduction in an area with a diameter of at least half the radius of the tip. If a higher deposition rate is obtained just below the tip's apex the deterministic movement of the tip should generate patterns narrower than the radius of the tip. The experimentation returned opposed results; a scan of an illuminated AFM tip over a substrate locally suppresses the laser-induced deposition of silver. This effect persists for some time

after scanning which derived in an easy to use "negative tone" patterning technique that has not been explored according to the authors' knowledge. Therefore a new technique to generate negative-tone silver patterns based on the suppression of photo-reduction by tip scanning during illumination has been demonstrated. The possible applications of this effect fall within the areas of mask repair, metal deposition, surface raman spectroscopy, and plasmonic sensors.

Chapter 4

EXPERIMENTAL SETUP

A diagram explaining the typical experimental setup used for this study is shown in figure 4.1. It consists of a liquid which is known to photoreduce to a metal when illuminated, a laser system to illuminate the liquid-substrate interface and the AFM table and tip to form the patterns. Figure 4.1 shows a microscope objective of focusing a laser beam on a glass sample containing the silver liquid precursor by means of an AFM liquid cell. An AFM tip is dipped in the precursor and scans the sample in contact mode for every experiment.

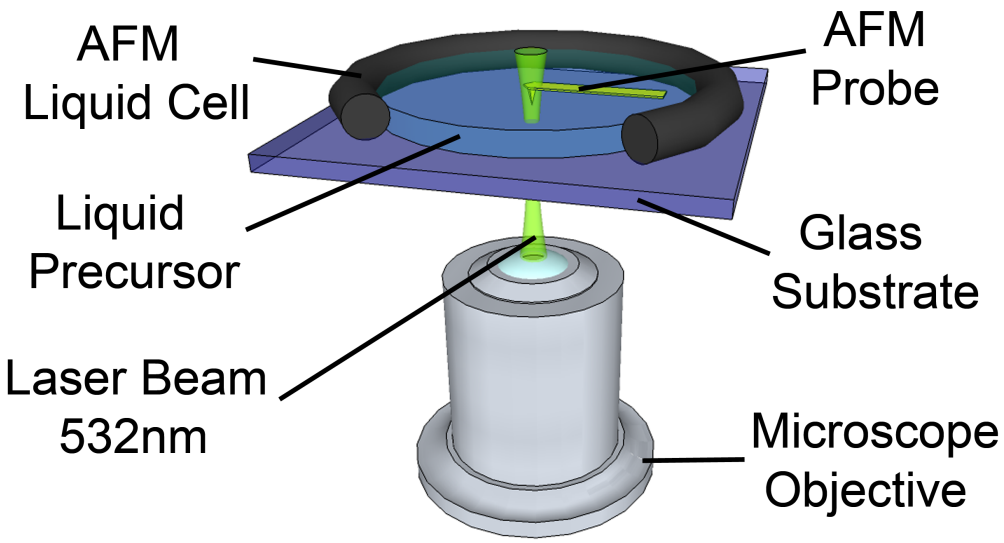

Figure 4.1: Experimental setup. A microscope objective with numerical aperture of 0.25 focuses a 532 nm laser beam on the interface between glass and a liquid precursor contained by an o-ring in the liquid cell. At the same time a gold coated AFM probe comes in contact with the glass over the area being illuminated.

4.1 Laser Illumination Systems

Three different illumination sources were used before settling with a final laser setup. The first experiments were made using pulsed lasers. Although these experiments did not provided conclusive results it is important to describe the systems for future references.

The initial experiments were done using a Spectra-Physics 337 nitrogen laser with a dye laser accessory. A Coumarin 480 dye from Exciton was used; hence the wavelength range obtained was from 453 nm to 523 nm. The pulse width of this laser is 4 ns and the maximum frequency is 20 Hz. However, for the experimentation the frequency was not set above 15 Hz. The maximum average energy measured at the output of this laser was 72 μJ. This output was coupled by means of a collimator to a multi-mode optic fiber and at the output of the final objective we had 23 μJ. The measured spot size was about 125 μm.

Another set of experiments was made with a Spectra-Physics GCR-170-30 q-switched Nd:YAG laser. This laser was set to emit a 532 nm wavelength. The pulse width of this laser is 7 ns and the maximum pulse frequency is 30Hz. The average energy specification for this laser is 300 mJ. However, the laser beam is passed through two beam splitters, 5 mirrors, an aperture with less than 1 mm in diameter, a polarizer, and the objective. At the end of the laser system the measured power was 1.37 mJ. When using this laser the power was set not greater than 49.5 μJ. The spot size at the output of this laser system is estimated in 20 μm of diameter.

The third laser source used for the experimentation was a continuous wave solid state green laser with a maximum power of 15 mW. This laser source was unstable with respect to the temperature and its power output changed greatly during the day. Hence, the need for a more stable source with a higher power output.

The final laser system used is described in figure 4.2. The laser system is in charge of providing a controlled illumination. The variables to control are the time and intensity that the liquid-substrate interface receives. The source is a diode pumped laser of 532 nm horizontally polarized and with a maximum power of 530 mW. An intensity control system is made using a half-wave plate (Thorlabs WPH05M-532) and a polarizer (Thorlabs GL5). Keeping the polarizer fixed while rotating the half-wave plate will change the power without changing the output polarization. The power controlled laser beam is then coupled to a single mode optic fiber (Thorlabs P1-488PM-FC-5) which maintains the polarization. This fiber gives the system the flexibility of changing the focus and the position of the laser beam without having to re-align all the optics. The beam at the output of the fiber is passed through a collimator (Thorlabs F260APC-A) and is oriented to a 30-70 beam

splitter (Thorlabs BST10). The percentages of transmitted and reflected power depend on the polarization of the incident beam; hence, the importance of the polarization maintaining optic fiber. In this case the incident wave is S polarized which divides the beam letting 15% being transmitted and 85% reflected. The weaker beam is measured at all time with a silicon and germanium photodiode sensor (Coherent OP-2 VIS). The stronger beam is aligned to a microscope objective with a numerical aperture of 0.25 used to focus the beam to a minimum spot of 4 μm in diameter.

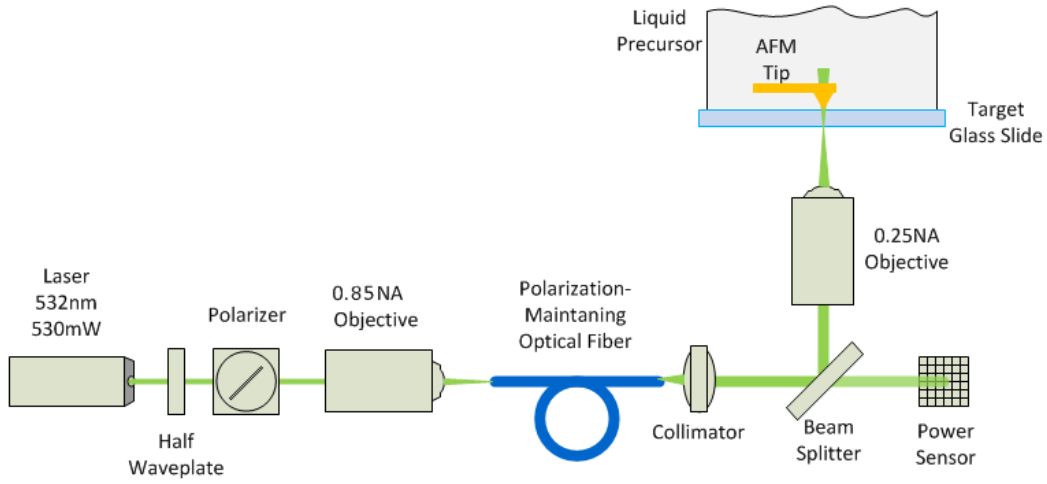

Figure 4.2: Laser System Descriptive Diagram. The complete laser system is shown. The intensity of the beam is attenuated by a half waveplate-polarizer pair, focused onto a single mode optic fiber with an objective with a numerical aperture of 0.85. The beam is collimated at the output of the fiber and divided by the beam splitter. The 15% of the beam is directed to a power meter while the 85% is focused on the glass-liquid interface by an objective with a numerical aperture of 0.25.

This laser system has been proved several times, its power is stable and the maximum value at the objective is 45mW. The power limit in this system is given by the single mode optic fiber which only stands 300 mW of input power. The coupling of the laser beam into the fiber optic has proven a challenge due to the coarse screws of the coupler used (Newport F-91-C1). However, the coupling objective used for this system has a numerical aperture of 0.85, and according to the calculations a better coupling can be obtained using a 0.65 NA objective. The proper objective was not available in the laboratory at the time the experiments were made.

4.2 Liquid Precursors

The photoreducing formula to form copper were obtained from Man'shina et al. and Kordás et al. [24, 23] Both authors use copper sulfate ($CuSO_4$), potassium sodium tartrate ($KNaC_4H_4O_6$), sodium hydroxide (NaOH) and formaldehyde (HCOH) in different proportions. Man'shina et al. suggests mixong 0.260 g of copper sulfate with 1.320 g of potassium sodium tartrate, 0.386 g of formaldehyde, 2.2 g of methanol and 2.5 g of water. In our system setup we decided to keep the solution at room temperature.

The gold precursor solution was obtained by mixing 1 mM of chloroauric acid ($HAuCl_4$) as proposed by Harada and Einaga [87] and 20 mM of sodium citrate ($NaC_6H_7O_7$) as it is known by its reducing properties.

The silver solution was obtained from Bjerneld et al. [88]. The liquid was made by diluting in water two salts, in our case fabricated by Sigma-Aldrich, sodium citrate ($NaC_6H_7O_7$) reference S4641, and silver nitrate ($AgNO_3$) reference 209139. Both salts are diluted in de-ionized water in a concentration of 1mM each. To homogenize the solution the bottle is dipped in a sonicator for 5 minutes. Being a solution that forms solid silver nanoparticles when exposed to light care has to be taken to cover the bottle from incidental illumination. The glass slide used as a sample was cleaned prior to every experiment by dipping it in acetone, isopropanol, and deionized (DI) water, sonicating it for five minutes in each case and doing one minute of microwave plasma etching after the sonications.

An Agilent 5500 AFM is used as a sample holder, liquid container, and for the tip movement. This model of AFM provides the option of having a liquid cell to do high resolution scans within liquids. In our case the liquid cell was used to contain the liquid precursor. The liquid cell consists of a plastic holder fixing an o-ring against the glass sample (see figure 4.3). This allows to place up to 0.8 ml of liquid in contact with an area of approximately 1.5 cm^2. The liquid cell has an opening where the scanning sensor and the tip can come in contact with the sample to make the image. We have used this liquid cell to hold the silver precursor and at the same time be able of doing a scan with the tip. Figure 4.3 shows a cut of each of the components of the Agilent 5500 liquid cell including the sample holder, glass slide, o-ring, and liquid cell. Note that the sample holder is providing

also screw holes to press the o-ring to the glass slide and the liquid cell. Additionally, the sample holder has to have a hole so that the laser beam can be applied to the sample.

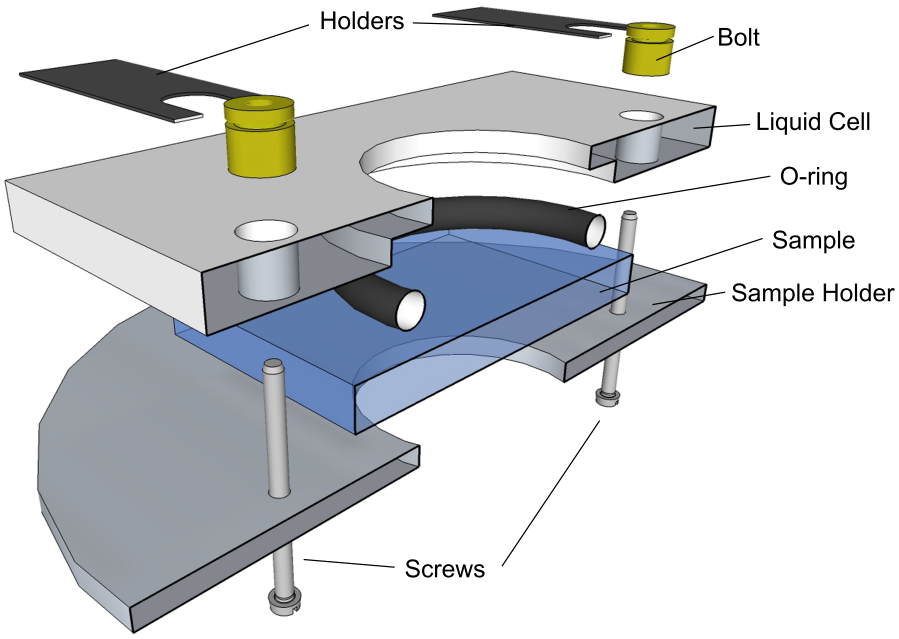

Figure 4.3: Liquid Cell Components. A silicone o-ring is pressed against the glass sample and the plastic liquid cell by means of screws attached to the sample holder.

For this study the AFM tip was moved around the illuminated area in contact mode, in this way the tip was always in contact with the sample. The force applied to the sample by the tip is given by the set point, set in all experiments to 0 V which translates to cantilever deflection of 0.25 μm and considering a force constant of the cantilever of 0.4 N/m the force applied to the surface will be around 0.1 μN. The potential difference between the tip and the sample holder is set to 0 V to avoid unwanted electrostatic effects. The tip used for the scans is a Budget Sensors' gold coated AFM tip (ContGB-G) which has a radius smaller than 25 nm.

Note that the concept of the system setup shown in figure 4.1 was maintained for every precursor and laser source tested. However, the AFM tip was not used with the Nd:YAG laser because it was immediately noticed that the energy was too high for the glass sample. This case is going to be explained more in depth in the following chapter.

Chapter 5

RESULTS AND DISCUSSION

5.1 Pulsed Laser Experimentation

Although this study shows results of silver patterning, the first materials we tried to deposit during the experimentation were copper and gold. It was thought that a specific wavelength was necessary to obtain the photoreduction. Hence, a pulsed dye laser was the best choice because of the flexibility in changing the wavelength. Several experiments were made with this illumination source trying different wavelengths and liquid precursors. However, after trying several times with different wavelengths/energy/precursor combination, and not getting any successful deposition, it was decided to maintain the wavelength fixed and use a more powerful laser system. This is when the experimentations with the Nd:YAG laser started.

The Nd:YAG experimentation was made also with a different precursor, one that was proven to reduce in silver nanoparticles. However, as soon as the Nd:YAG laser system was set we noticed that the energy generated by this laser was going to be too high. The focused energy, without any sample near it, was able to break-down air at the focal point. Even with a minimum power setting (20 μJ) the glass sample was melting. Some nanoparticles were observed in the scanning electron microscope (SEM) images taken from these experiments, however, the little deposition obtained was affected greatly by the destruction of the glass sample due to the excessive pulse energy. After looking more closely to the Surface Enhanced Raman Scattering research done by Bjerneld et al. [88], where they obtained a successful deposition using a 3 mW continuous wave laser illuminating the sample during 15 seconds, it was decided to switch to a continuous wave laser. Switching to the continuous wave laser was a crucial change in our deposition success.

5.2 Continuous Wave Laser Experimentation

After making the laser source type change to continuous wave, the deposition of silver on the glass substrate was easily achieved even with a not so stable or powerful solid state laser. An illumination of the substrate and the solution with an intensity of approximately 4.3 kW/cm^2 during 15 seconds generated a highly deposited area like the one shown in figure 5.1.

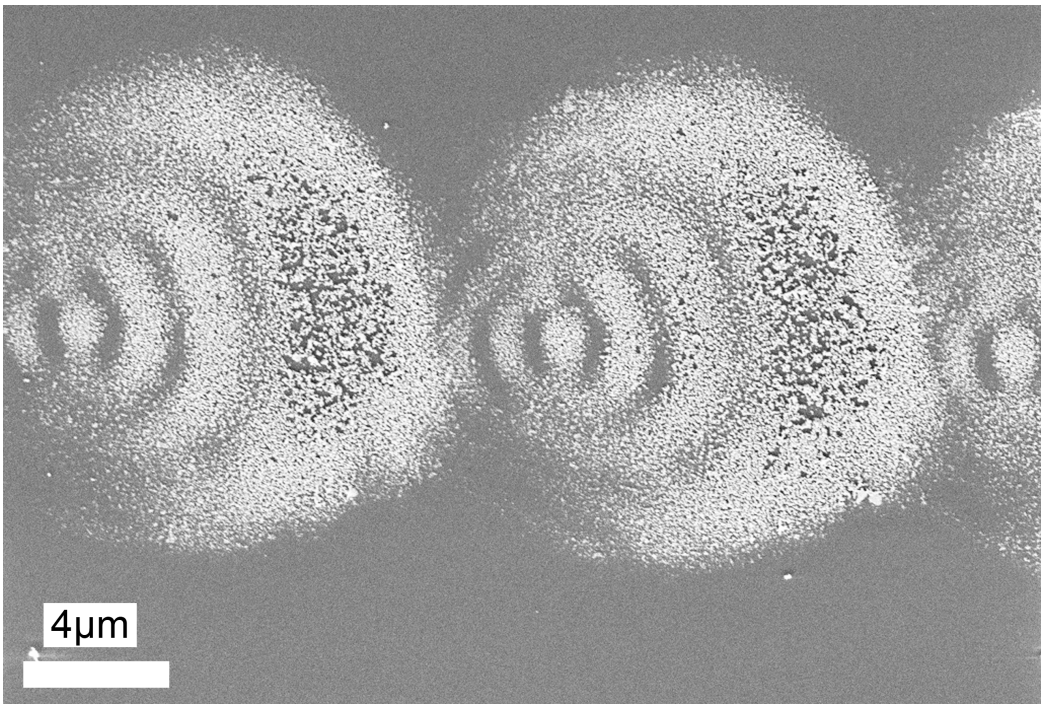

Figure 5.1: Silver deposition on glass substrate formed after illumination with the solid state laser source. A 10 mW continuous wave solid state laser was focused to a diameter of 12μm on a liquid-ITO glass interface. The illumination time for each deposition was 15 seconds. The calculated intensity is over 4.3 kW/cm^2.

The figure 5.1 shows two circular but not homogeneous depositions. The irregular density and shape of the deposition is due to the hot spots of the laser source and its non-idealities. This was one of the reasons why a single mode optic fiber was wanted in the final system setup. This type of fiber would help us in the cleaning of the laser source removing any hot spots and providing a clean gaussian beam. Once the laser system was proven to generate repeatable depositions, the AFM tip was brought in place to try the enhancement experimentation.

5.2.1 Basic Illumination Experiment

As it was mentioned in section 4.1 the beam waist at the focal point of the laser system is about 4 μm. In order to obtain a deposition area greater than 500 μm^2 (at least five times the size of the scanned area) the laser beam was not focused precisely at the substrate-liquid interface but a few micrometers before. An SEM image (obtained using a Hitachi S4300) of a silver deposition is shown in figure 5.2. The deposition in figure 5.2 was obtained with a 5 minute illumination at about 20.5 W/cm^2. This image shows several irregularly shaped particles of sizes from 50 to 500 nm. The space between them also changes but for the most part is not greater than 500nm. This behavior is only observed in the center of the illuminated area; the peripheral regions (not shown in the figure) that receive less power are not as densely spaced.

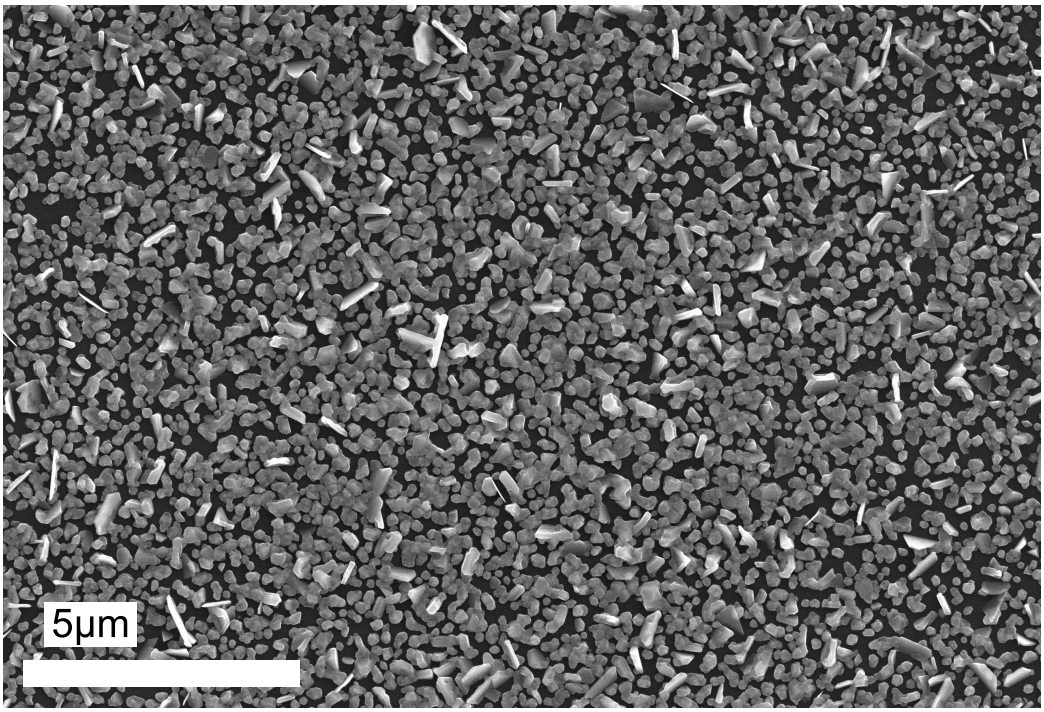

Figure 5.2: Silver deposition on glass substrate formed after illumination. Silver nanoparticles as deposited on a glass substrate after a 5 minute illumination at 21 W/cm^2.

To verify the composition of the silver particles deposited, an Energy Dispersive X-ray Spectroscopy (EDS) was conducted on several samples. The EDS data, obtained using a Hitachi S-3200N, is shown in figure 5.3. The measurements are taken with an Evex silicon lithium detector. The silicon (Si), sodium (Na), oxygen (O) and calcium (Ca) peaks are

present due to the glass slide used as a substrate. The dashed red curve shows the spectrum for a not deposited area from the substrate. The blue curve shows the spectrum for a densely deposited area. The deposited area shows two peaks due to Silver (Ag) presence. From the three Silver (Ag) peaks obtained, one is present in both curves probably due to residues of the silver nitrate ($AgNO_3$) salt, and the other peaks are only present in the deposited section of the sample. This confirms that the particles are mostly made of silver.

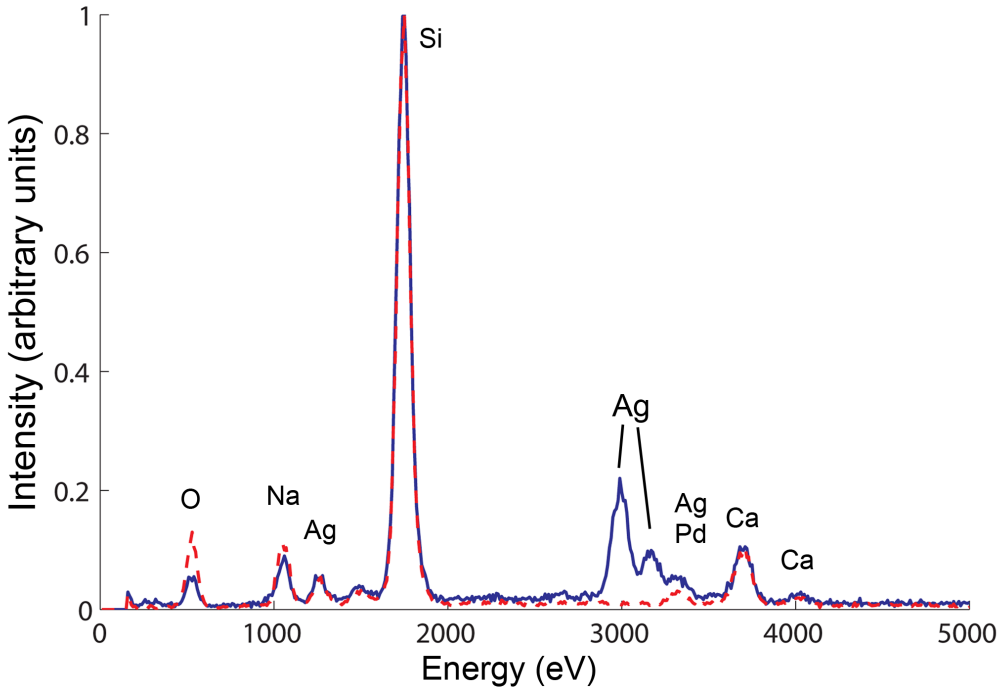

Figure 5.3: EDS data for a deposited area and a not deposited area from the same sample. The dashed red curve shows the spectrum for a not-deposited area from the substrate. The solid blue curve shows the spectrum for a densely deposited area. The deposited area shows additional peaks due to the presence of silver. Other peaks are attributed to the glass substrate.

5.2.2 Scanning During Illumination Experiment

As it was mentioned in section 2.3, the plasmonic principles suggest an intensity enhancement and confinement at the apex of the tip. This enhanced electromagnetic field should have generated greater deposition (larger density or size of the particles) in the area scanned. The obtained result was completely different to the one expected as it is shown in figure 5.4. The image in this figure was taken after illuminating the sample with a focused 532 nm

laser beam, for 5 minutes at about 20.4 W/cm^2, while a 10 μm by 10 μm area is scanned at a speed of 16.7 μm/s. The image shows an area of 10 μm by 10 μm with a clearly reduced deposition due to the scanning.

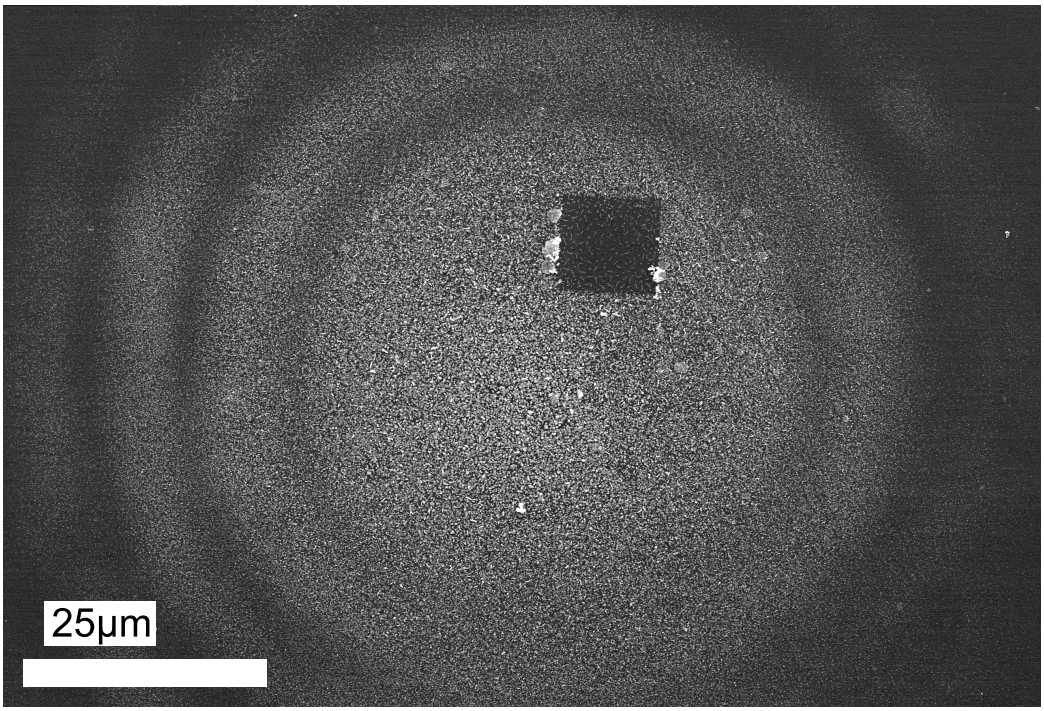

Figure 5.4: Silver deposition on glass substrate formed during illumination and scan. Deposition of silver nanoparticles and cleared area obtained when illuminating the sample while scanning a 10 μm by 10 μm area. The deposition spot size is approximately 80 μm while the square cleared area has exactly 10 μm of side. The scan speed is 16.7 μm/s. The number of particles inside the area is clearly reduced by the scanning. This deposition was formed with a 5 minutes illumination at 21 W/cm^2.

There are several possible explanations for this reduction of deposition but the two most probable are: not having an ideal angle of incidence of the laser, and the use of contact mode during the scanning. The laser setup is designed such that the incident illumination is practically at a 0° angle with respect to the substrate normal. As several authors have reported previously, a greater field enhancement is obtained in a tip-particle geometry for the electromagnetic component that is in the same direction as the tip (normal to the substrate) [9, 89]. In our experiment only a small component in this direction is present due to the focusing of the laser beam. The enhancement of such component is probably negligible. Along with the first possibility, the scan mode of the AFM sensor is contact mode. As it was mentioned before, in contact mode the tip is in contact with the surface

of the sample at all times, in this way the lateral force the tip applies to the newly formed particles is enough to detach them from the substrate setting them at the sides of the scanned area and/or leaving them suspended in the solution. Several investigations have been made by different authors to show that manipulation of nanoparticles is easily achieved with a moving AFM tip [4, 90].

One might first assume that this result can be explained by simple mechanical removal of the deposits by the tip. That is, even if the tip enhances deposition, the lateral force applied by the scanning tip is sufficient to remove deposited particles. As we state below, by scanning the particles after deposition, sufficient lateral forces are present. However, a purely mechanical cause does not explain why the suppression of deposition is uniform. One would expect that regions scanned earlier in the process, e.g. the top of the cleared region in figure 5.4, would refill with material while the remainder of the scan is being executed. Such refilling does not occur, even during scans that require far longer than the deposition process, and a more complex mechanism must be sought to explain the phenomenon.

Thus, we conducted a series of experiments to elucidate the suppression mechanism. First, we show that suppression of deposition persists for at least tens of minutes, even during subsequent laser exposure in the absence of a scanning tip. This suggests either a tip-induced surface modification or preferential deposition on previously deposited particles. However, we rule out a purely tip-based modification by showing that pre-scanning the surface before illumination, rather than during illumination, has little effect. We also show, using an optical projection approach, that preferential deposition on previously deposited material does not explain the phenomenon. Thus, the substrate surface is modified only by simultaneous illumination, scanning, and perhaps partial deposition. In support of this, we show that the suppression of deposition is reversible by simply exposing the substrate to atmosphere. Ultimately, this series of experiments narrows down the cause of suppressed deposition to a persistent, but reversible, surface modification which could be attributed to the removal of nucleation sites by some combination of mechanical, photothermal, or photochemical processes. The result is a new "negative tone" patterning technique that directly deposits a functional material.

5.2.3 Scanning After Illumination Experiment

To verify if the contact strength used is able to remove particles from the substrate we illuminated a sample and scanned it *after* obtaining deposited particles. An image of one of these experiments is shown in figure 5.5. It turns out that although the tip indeed is able to move particles, only some of the particles were removed. It is possible that the lateral force applied to the particles by the tip after the illumination is finished is not as strong as during the illumination is made. This can be an entirely mechanical effect. The tip could not be able to be in full lateral contact with the particles because the film-like characteristics of the deposition do not allow the deeper penetration of the tip. Or it can be that the illumination and the heating effects over the tip and over the particles will reduce the adhesion of the particles to the substrate. Both of these explanations verify our initial thought that the illumination during the scan is essential in the deposition reduction.

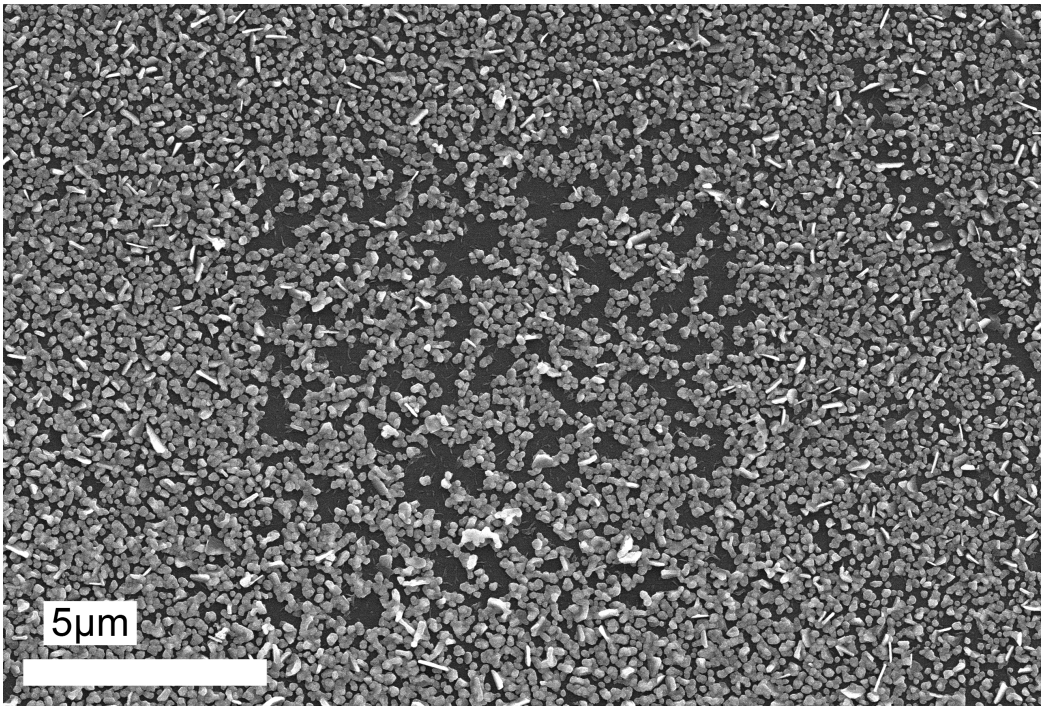

Figure 5.5: Silver deposition on glass substrate after doing a scan following an illumination. Deposition of silver left after scanning a 10 μm by 10 μm square, minutes after illuminating the sample without scanning. The illumination was made during 5 minutes with a 20 W/cm^2 intensity. The scan removed some of the particles recently deposited but most of the particles are still attached to the substrate.

Note, in figure 5.4, that the size of the cleared area is very similar to the size of the area scanned (10 μm by 10 μm). However, another experiment showed that a laser illumination of just two minutes leaves a considerable amount of particles deposited in the sample. The top region of the cleared area shows a much smaller quantity of particles. Being scanned in the first seconds this region has been exposed to illumination of at least four minutes after the tip scanned it; the deposition though, is not as much as we expected from a four minute illumination. This detail prompted us to study the behavior of scanned regions and determine if the scanning is indeed removing the deposited particles and preventing future deposition in the scanned area.

5.2.4 Second Illumination After Scanning During Illumination

We first need to confirm that scanning during illumination suppresses deposition for some time after the tip is removed. A convenient experiment to confirm this is to scan an area during illumination for five minutes; after the scan is finished, another illumination of five minutes takes place over the same area but without scanning. Figure 5.6 shows the results of illuminating the sample while a 10 μm by 10 μm area is scanned at a speed of 16.7 μm/s. As expected, the quantity of particles inside and outside of the scanned area is greater compared to the image in figure 5.4 where there is no second illumination. The number of particles inside the scanned area though, is much lower than what would be expected in a first illumination without scanning experiment.

The results seen in figure 5.6 suggest that either the scanning tip prevents deposition by modifying the surface, or that any subsequent deposition occurs preferentially on the particles deposited during the first illumination.

5.2.5 Scan Before Illumination Experiment

To determine whether the tip alone modifies the surface, an experiment was conducted where the surface of the substrate was scanned *before* any illumination. Afterwards the same area was illuminated in the absence of the tip. In this case, the scanned area was re-deposited with silver, and the deposit appeared much the same as the surrounding area.

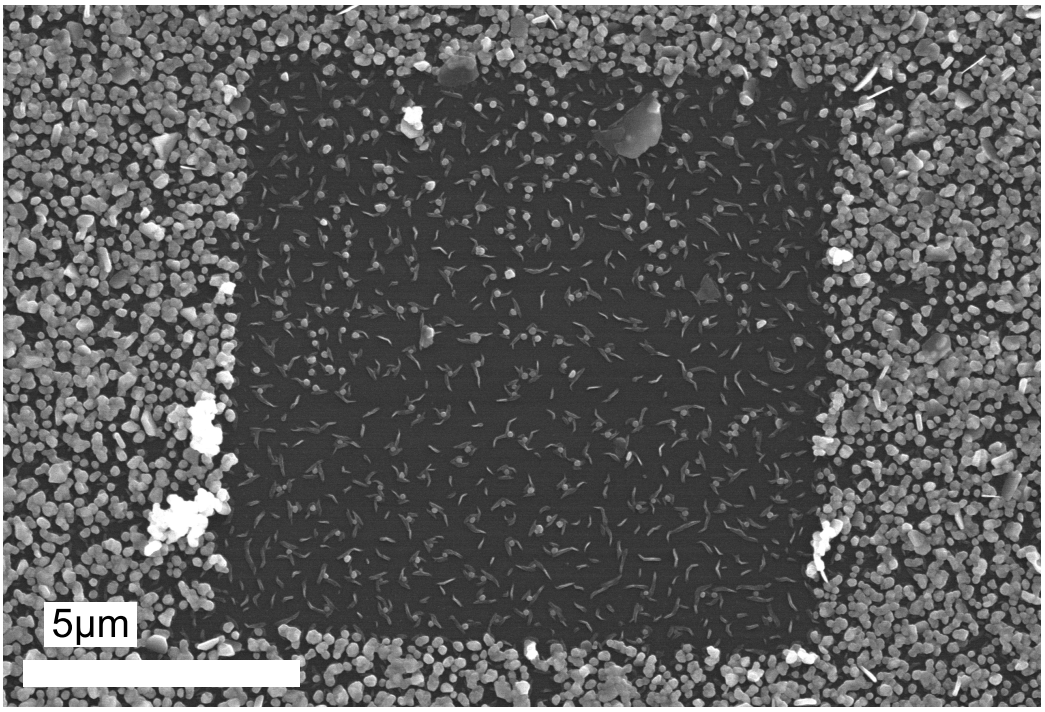

Figure 5.6: Silver deposition on glass substrate formed after two illuminations, the first one done during scanning. The sample is illuminated while a 10 μm by 10 μm area is scanned at a speed of 16.7 μm/s. As expected, the quantity of particles inside and outside of the scanned area is greater compared to the image in 5.4 where there is no second illumination. The number of particles inside the scanned area, though, is much lower than what would be expected in a first illumination without scanning experiment.

In three out of four experiments the deposition was so uniform that it was not possible to identify in the SEM images any difference between the area scanned and the other deposited areas. In one of the pictures a difference in density was spotted however the scanned area was not as clear of depositions as in the experiments where the scan was made during the illumination. This suggests that suppressed deposition only occurs when the area is scanned and illuminated simultaneously.

5.2.6 Double Illumination With and Without Mask

Another possible explanation for the lack of deposition in a subsequent illumination argues that the silver particles created in the second illumination could be deposited on top of previously deposited particles more easily than on top of a cleared substrate. An illumination was made using a mask to form a clean area (see figure 5.7 (a)); next, another clean area was made with the same mask and then a second illumination was made on top of the previous one to see if there was any deposition suppression in the non-deposited area. The formerly clean area was deposited without any suppression (see figure 5.7 (b))proving then that a scan with an illuminated tip is essential in order to produce any type of deposition reduction.

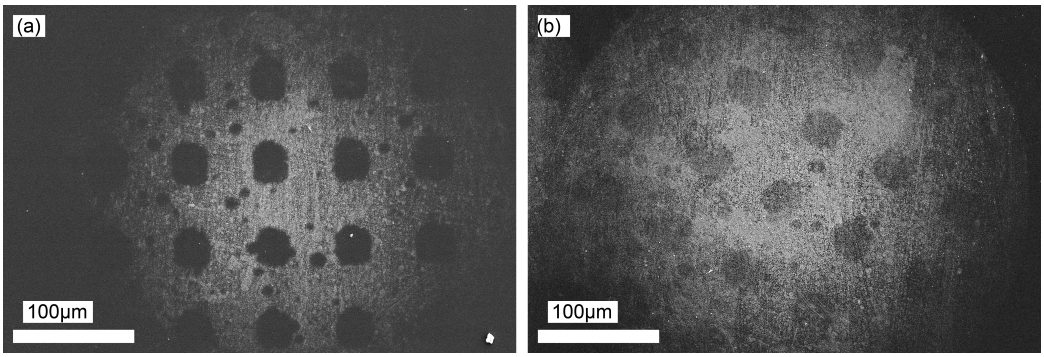

Figure 5.7: Comparison of re-deposition using a mask instead of a scanning tip for preventing deposition. (a) SEM image of the deposition of silver with clean areas generated using a mask to block the laser illumination. (b) SEM image of the results of a double illumination; the first illumination is made using a mask and the second illumination is made without the mask. It is shown in figure (b) that the second illumination (without the mask) induces deposition in every region, regardless of whether the region is already covered in deposits or not.

5.2.7 Reversibility of the Suppression of Deposition

Two additional experiments were performed in order to observe the reversibility of the suppression of deposition. In both of these experiments the first step was to do an initial illumination while the tip scanned the area for five minutes, thus creating a deposition spot with a cleared 10 μm by 10 μm area. After this initial scan during illumination the two experiments differ. In the first experiment, the liquid precursor was replaced without exposing the sample to the atmosphere; in the second experiment the sample was washed with DI water and dried by means of blown air, and then a second illumination with a similar intensity was done but without a scanning tip.

For the first experiment, the results were very similar to the ones obtained when a second illumination without scanning was done without changing the solution (cf. figure 5.6). This result ruled out a simple depletion of silver or citrate ions near the deposit in the static solution. This was not surprising given that diffusion alone should be sufficiently fast to replenish the region on a time scale far shorter than the duration of these experiments.

The second experiment results are shown in figure 5.8; the second illumination (without scanning) generated new deposition even inside the previously cleared area. The SEM image in figure 5.8 can be compared with that shown in figure 5.6. Both experiments have a second dose of illumination after a scan-during-illumination procedure; however, the deposition inside the 10 μm by 10 μm scanned area seen in figure 5.8 is much greater than the one seen in figure 5.6. It can be said that the number and size of the particles inside the scanned area for the illumination after washing the sample is similar to the particles surrounding the scanned area in figure 5.4. This is clear evidence that the exposure to the atmosphere returned the sample's surface to the original state. Any illumination after the sample washing will generate the same rate of growth in the previously scanned area as if the area had never been processed.

5.2.8 Increasing the Suppression of Deposition

With the certainty of the suppression, it is convenient to question of the possibility of reducing the deposition during the second illumination much more. To answer this, an experiment was made in which a same area was scanned several times while being illuminated,

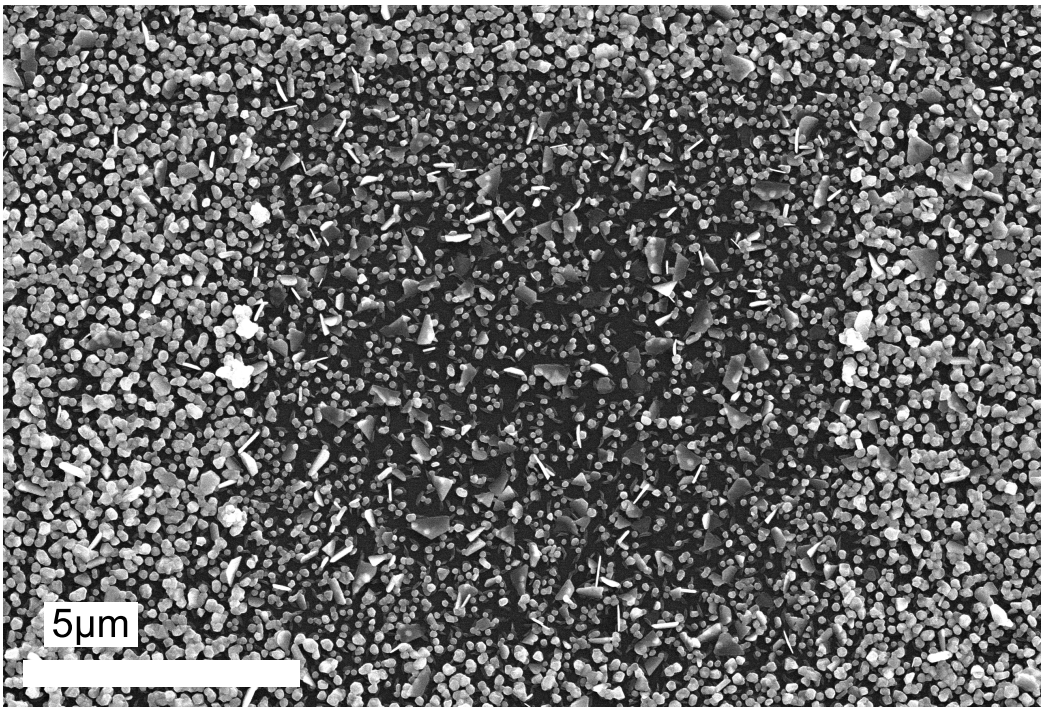

Figure 5.8: Silver deposition after wash and second illumination. Silver deposits on a glass slide after an experiment where the slide was illuminated while a 10 μm by 10 μm area was being scanned, then the sample was washed with DI water and next the same spot was illuminated again. The scanned area is visible because the particles at the side are larger, however, the particles where the scan was made are similar in size and quantity to a regular one-illumination deposition.

next an illumination without scanning was made. If more scans during illumination can suppress even more the deposition, there will be a difference between a sample scanned one time and a sample scanned three, five and eight times. Figure 5.9 shows sliced images of the same region of the scanned area. The left section shows the deposition on a glass slide after one scan during illumination and another five more minutes of illumination. The right section of the figure shows the deposition after three scans during illumination and another five more minutes of illumination. There are clear differences in the size and quantity of the particles inside the scanned area. Note that the particles surrounding the scanned area in the right side (three scans during illumination) are larger and greater in number than the particles surrounding the area in the left side (one scan during illumination). Indeed the right side of the figure shows a smaller number of particles with smaller size than the left side of the picture.

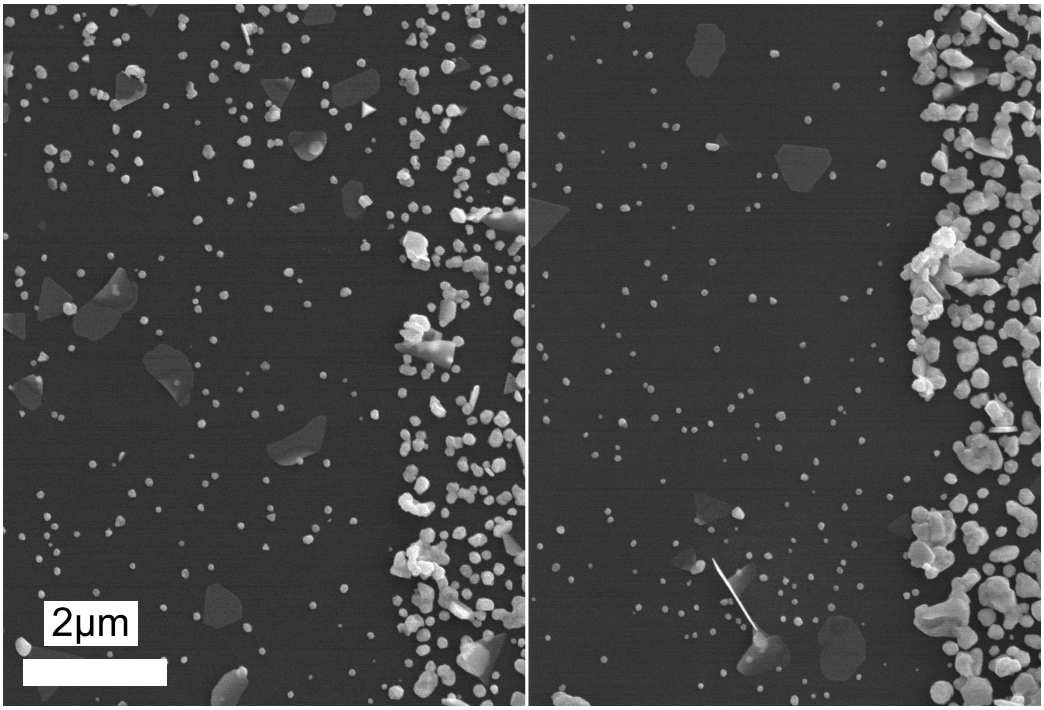

Figure 5.9: Silver deposition after one scan versus three scans. Sliced pictures of the same region of the scanned area. The left section shows the deposition on a glass slide after one scan during illumination and another five more minutes of illumination. The right section of the figure shows the deposition after three scans during illumination and another five more minutes of illumination. Qualitatively there are clear differences in the size and quantity of the particles inside the scanned area, however, the statistics are not as conclusive.

Although this experiment is visually clear in some sections of the suppressed areas, the particle statistics returned a number of 595 grains of an average of 61 nm in diameter for the experiment with one scan during illumination, against 553 grains with a diameter of 47 nm in average for the experiment with three scans during illumination. These results although interesting are not conclusive enough. Unfortunately the experiments of scanning during illumination five or eight times, which could provide more conclusive information, presented a major difficulty in realization. After the third scan during illumination the particles surrounding the scanned area become too large and the scanned area even though cleared, becomes too irregular in shape. It is believed that the tip starts to accumulate too many silver deposits losing its sharpness and forming a thick irregular metallic broom that spreads the already deposited particles all over the illuminated area.

5.2.9 Formation of Silver Nanopatterns

We have shown that the growth reduction at the second illumination is due to the contact of the sample with the illuminated tip. Also, the experiment in which the surface characteristics are reset shows that the mechanism of growth is much more complicated than initially expected. Nonetheless, negative-tone patterns can be made using this technique. Figures 5.12 to 5.14 demonstrate the feasibility of generating patterns smaller than 10 μm by 10 μm squares.

To form a useful pattern the tip should move in a deterministic manner during illumination. To that end the PicoLith tool, included in Agilent's PicoView 1.8.2 software, is used to develop simple patterns and it is connected to the controller of the piezoelectric device that controls the movement of the AFM tip. A pattern can be generated by illuminating an area of the substrate and scanning the regions where it is not desired to have silver. These patterns will persist even during subsequent illumination as long as the sample is not washed. To verify the patterning technique and understand its quality and limitations several simple patterns were made. Figures 5.10 and 5.11 show the versatility of the PicoLith tool.

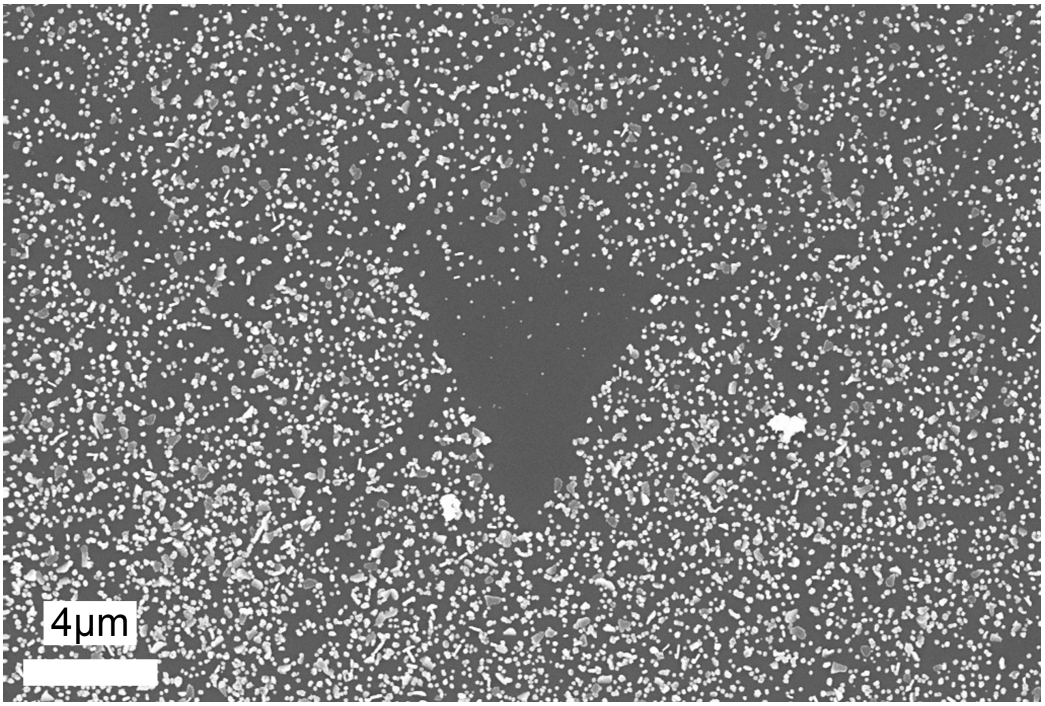

Figure 5.10: Triangular pattern. Silver deposits on a glass substrate made with laser illumination while scanning an inverted isosceles triangle with a base of 8.8 μm, and sides of 9.8 μm.

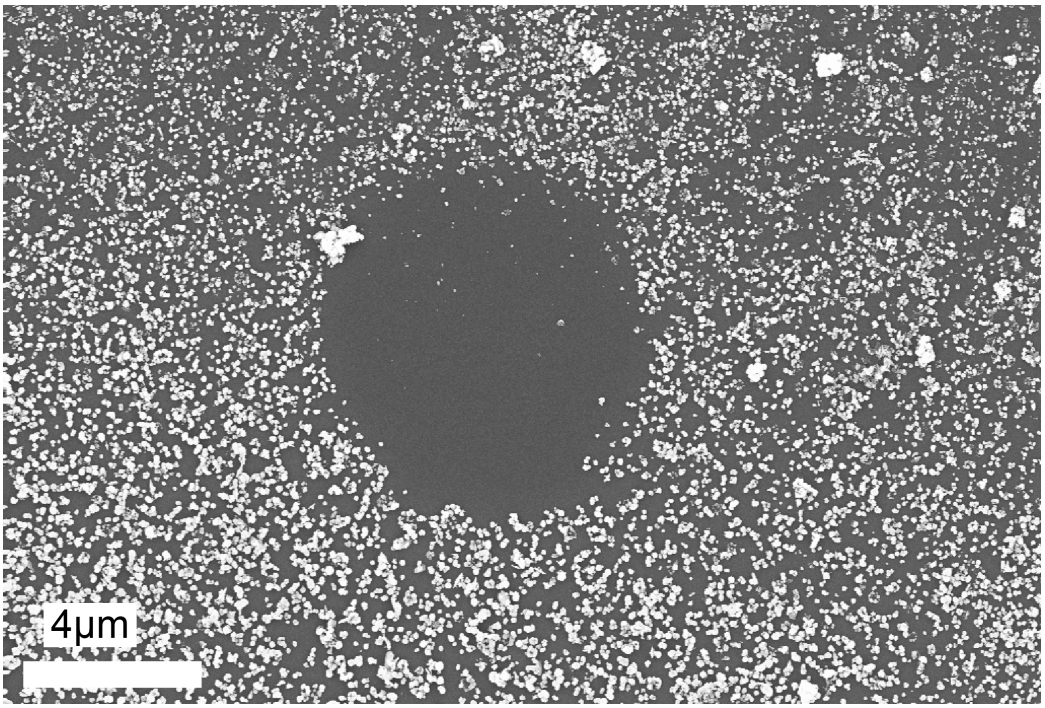

Figure 5.11: Circular pattern. Silver deposits on a glass substrate made with laser illumination while scanning a circle of 3.6 μm in radius.

The most promising results were obtained when patterning a series of bands of width equal to 2 μm, 1 μm, and 0.5 μm, separated by the same width of deposited bands. Figures 5.12, 5.13, and 5.14 show the SEM image of the patterns formed when the scanning of bars with width of 2 μm, 1 μm, and 0.5 μm respectively. Each of the patterns was formed horizontally and vertically to verify if the scan order had any effect on the patterns. The PicoLith software was used to move the tip from top to bottom and from left to right. The speed was such that the scan of the bands was done in 5 minutes, which will assure that the illumination dose was the same as in the previous experiments. Deposits are present mostly on the areas that were not scanned, while the scanned areas show a great reduction in the quantity of silver particles.

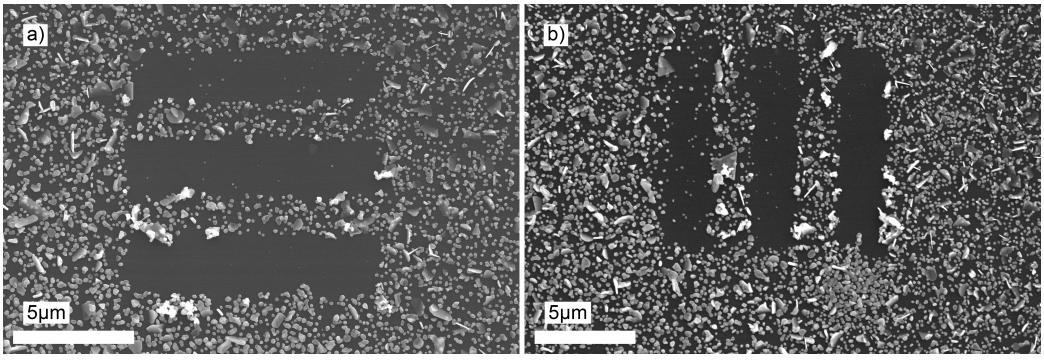

Figure 5.12: Patterns of horizontal and vertical two micrometer bars. Silver deposits on a glass substrate made with laser illumination while scanning bands of 2 μm width spaced by 2 μm. (a) Horizontal bars scanned from top to bottom. (b) Vertical bars scanned from left to right. Each bar is scanned from top to bottom.

Aside from the large gaps of regions without silver, which can be optimized by varying the dose of illumination, the patterns formed by the scanning bands of 2 μm and 1 μm width were generated correctly. The width of the cleared sections was not exactly 2 μm and 1 μm, almost in every section of the bands the cleared sections are wider than the deposited sections. The patterns generated with the 0.5 μm wide bands presented high irregularities, sections without deposits and large particles in the supposedly cleared area. Most of the particles present in these experiments are relatively large (see 5.14). The large size of the particles, some of which are at least 250 nm in diameter, limit the generation of narrower

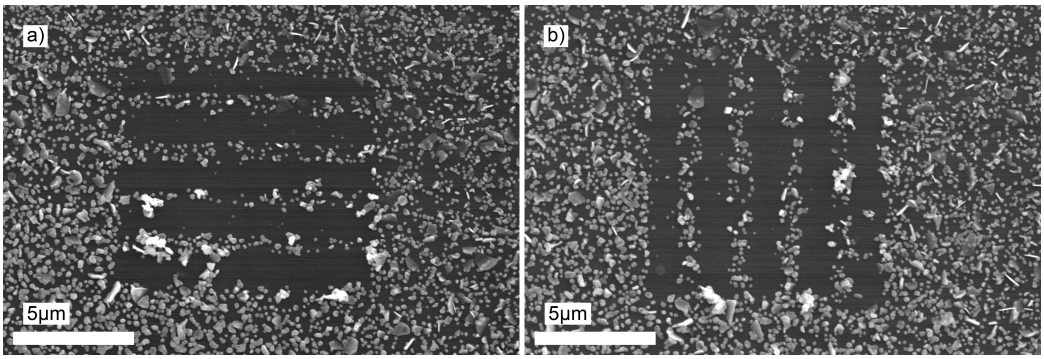

Figure 5.13: Patterns of horizontal and vertical one micrometer bars. Silver deposits on a glass substrate made with laser illumination while scanning bands of 1 μm width spaced by 1 μm. (a) Horizontal bars scanned from top to bottom. (b) Vertical bars scanned from left to right. Each bar is scanned from top to bottom.

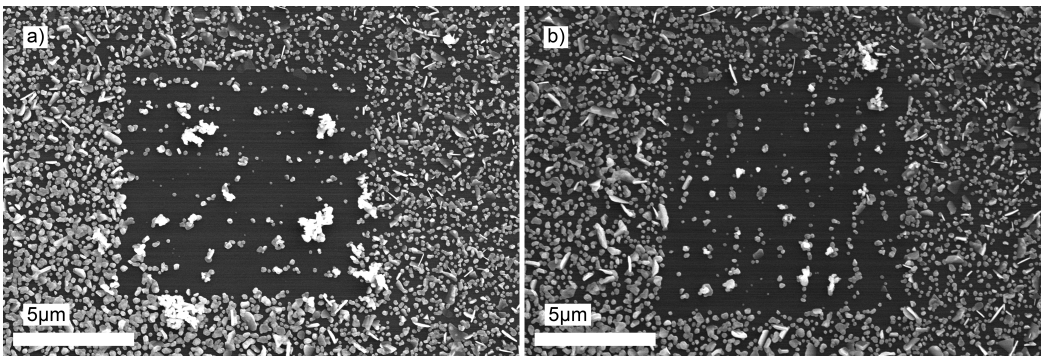

Figure 5.14: Patterns of horizontal and vertical half of a micrometer bars. Silver deposits on a glass substrate made with laser illumination while scanning bands of 0.5 μm width spaced by 0.5 μm. (a) Horizontal bars scanned from top to bottom. (b) Vertical bars scanned from left to right. Each bar is scanned from top to bottom.

patterns because the tip drags these large particles and they bump into other particles to form large clusters. These clusters can move to the cleared area or generate large gaps in the deposited areas. The method is currently limited with respect to density of the deposited areas and size of the particles; however it is expected that these obstacles can be overcome with a detailed study of illumination dose and precursor chemistry.

Chapter 6

CONCLUSIONS

In summary, enhanced photodeposition near a metallic scanning probe tip was not observed for the narrow range of conditions considered here. Mechanical displacement of the particles by the tip may counteract the enhanced deposition; however, the illumination conditions were also not favorable to produce a large field enhancement. For future efforts the angle of incidence should be tuned to obtain maximum field enhancement, and the tip should not be in contact with the sample. The most important effect observed in this study was the suppression of deposition after scanning the tip during illumination. Neither scanning the tip in the absence of illumination nor pre-depositing material nearby reproduces the effect. The clearing effect lasts at least tens of minutes while the sample remains covered by a liquid; however after the sample is washed and dried silver can be deposited again with the same rate. One speculative explanation for these results is that particles are deposited, removed by the scanning tip, and that in the process the defect, impurity, or contaminant that served as a nucleation site is also removed. If so, the experiments also suggest that the nucleation sites can be reintroduced by exposure to atmosphere. Regardless, the three simplest mechanisms have been ruled out and a solid foundation for future work has been established.

The effects described above can form the basis for a method for negative tone, tip-based patterning. However, more refinement is required to produce truly nanoscale patterns. Developing photoinduced deposition processes that produce films containing smaller, denser particles and alternative materials will be an important first step. If successfully extended, the technique could provide a new approach to nanoscale rapid prototyping and semiconductor mask repair. Regardless, suppression of photoinduced deposition by a scanning probe can be counted among a small group of nanopatterning approaches that directly deposit functional materials in a single step.

Chapter 7

FUTURE WORK

As it was mentioned in the conclusions (chapter 6) we will need to refine this technique in order to be able to produce nanoscale patterns.

One of the characteristics of the deposition to improve will be to increase the density of the deposited film. An enhanced density will allow the elaboration of continuous patterns, an essential property of the film if it is going to be used in mask generation or to create conductive nanopatterns. Another important factor that can alter the quality of the pattern is the size of the deposited nanoparticles. As explained in section 5.2.9 a smaller size of the formed nanoparticle increases the possibility of generating narrower patterns. Additionally, a large particle will increase the probability of having irregular edges in the patterns. Obtaining smaller particles will reduce the dragging of the particle by the tip. These two improvements can be achieved by having more precise control in the intensity and time of the illuminations.

Considering applications in the mask repair industry, a deposition of different materials will be necessary. Some of the materials used in masks nowadays are chrome, alloys of molybdenum and silicon, aluminum nitride, titanium nitride and tantalum boron nitride depending in the illumination wavelength [91, 92].

An obvious method of deposition of nanopatterns to continue exploring is the enhancement in deposition due to the plasmonic field enhancement at the apex of the tip. Although in this study an interesting and useful behavior has been investigated, the original hypothesis has not been proved. To try to develop the plasmonic nanopatterning technique, experiments will have to reproduce the ideal conditions for field enhancement. The illumination has to be done with an optimal angle of incidence and the tip should not be in contact with the substrate to eliminate mechanical removal effects. Tapping mode could be appropriate

for this new set of experiments, because the amplitude can be set so the tip does not contact the surface of the sample being scanned.

REFERENCES

[1] H. Y. Lee, H. K. Park, Y. M. Lee, K. Kim, and S. B. Park, "A practical procedure for producing silver nanocoated fabric and its antibacterial evaluation for biomedical applications," *Chemical Communications*, no. 28, pp. 2959–2961, 2007.

[2] W. F. van Dorp, X. Zhang, B. L. Feringa, J. B. Wagner, T. W. Hansen, and J. T. De Hosson, "Nanometer-scale lithography on microscopically clean graphene," *Nanotechnology*, vol. 22, no. 50, p. 505303, 2011.

[3] E. Betzig and J. K. Trautman, "Near-field optics: microscopy, spectroscopy, and surface modification beyond the diffraction limit," *Science*, vol. 257, no. 5067, pp. 189–95, 1992.

[4] T. R. Ramachandran, C. Baur, A. Bugacov, A. Madhukar, B. E. Koel, A. Requicha, and C. Gazen, "Direct and controlled manipulation of nanometer-sized particles using the non-contact atomic force microscope," *Nanotechnology*, vol. 9, no. 3, pp. 237–245, 1998.

[5] R. D. Piner, ""dip-pen" nanolithography," *Science*, vol. 283, no. 5402, pp. 661–663, 1999.

[6] G. Mie, "Articles on the optical characteristics of turbid tubes, especially colloidal metal solutions," *Annalen Der Physik*, vol. 25, no. 3, pp. 377–445, 1908.

[7] M. Quinten, "Local-fields and poynting vectors in the vicinity of the surface of small spherical-particles," *Zeitschrift Fur Physik D-Atoms Molecules and Clusters*, vol. 35, no. 3, pp. 217–224, 1995.

[8] I. Notingher and A. Elfick, "Effect of sample and substrate electric properties on the electric field enhancement at the apex of spm nanotips," *Journal of Physical Chemistry B*, vol. 109, no. 33, pp. 15699–15706, 2005.

[9] Z. Yang, J. Aizpurua, and H. Xu, "Electromagnetic field enhancement in ters configurations," *Journal of Raman Spectroscopy*, vol. 40, no. 10, pp. 1343–1348, 2009.

[10] X. Chen and X. Wang, "Near-field thermal transport in a nanotip under laser irradiation," *Nanotechnology*, vol. 22, no. 7, p. 075204, 2011.

[11] G. M. Huda, E. U. Donev, M. P. Mengüç, and J. T. Hastings, "Effects of a silicon probe on gold nanoparticles on glass under evanescent illumination," *Opt. Express*, vol. 19, no. 13, pp. 12679–12687, 2011.

[12] A. Hartschuh, "Tip-enhanced near-field optical microscopy," *Angew Chem Int Ed Engl*, vol. 47, no. 43, pp. 8178–91, 2008.

[13] M. V. Cañamares, J. V. Garcia-Ramos, J. D. Gomez-Varga, C. Domingo, and S. Sanchez-Cortes, "Ag nanoparticles prepared by laser photoreduction as substrates for in situ surface-enhanced raman scattering analysis of dyes," *Langmuir*, vol. 23, pp. 5210–5215, 2007.

[14] B. Radha, S. Kiruthika, and G. U. Kulkarni, "Metal anion-alkyl ammonium complexes as direct write precursors to produce nanopatterns of metals, nitrides, oxides, sulfides, and alloys," *Journal of the American Chemical Society*, vol. 133, no. 32, pp. 12706–12713, 2011.

[15] V. M. Sundaram, A. Soni, R. E. Russo, and S. B. Wen, "Analysis of nanopatterning through near field effects with femtosecond and nanosecond lasers on semiconducting and metallic targets," *Journal of Applied Physics*, vol. 107, no. 7, 2010.

[16] E. A. Hawes, J. T. Hastings, C. Crofcheck, and M. P. Menguc, "Spatially selective melting and evaporation of nanosized gold particles," *Opt Lett*, vol. 33, no. 12, pp. 1383–5, 2008.

[17] S. J. Henley and S. R. P. Silva, "Laser direct write of silver nanoparticles from solution onto glass substrates for surface-enhanced raman spectroscopy," *Applied Physics Letters*, vol. 91, no. 2, pp. 023107–3, 2007.

[18] J. H. Kim, B. S. Shin, J. S. Ko, J. S. Go, K. R. Kim, and Y. K. Jeong, "Direct micro fabrication of flexible copper clad laminate using 355 nm uv laser," *Japanese Journal of Applied Physics*, vol. 47, no. 8, pp. 6883–6886, 2008.

[19] M. Sakamoto, M. Fujistuka, and T. Majima, "Light as a construction tool of metal nanoparticles: Synthesis and mechanism," *Journal of Photochemistry and Photobiology C: Photochemistry Reviews*, vol. 10, no. 1, pp. 33–56, 2009.

[20] T. C. Chong, M. H. Hong, and L. P. Shi, "Laser precision engineering: from microfabrication to nanoprocessing," *Laser & Photonics Reviews*, vol. 4, no. 1, pp. 123–143, 2010.

[21] R. Deng, J. Li, H. K. Kang, H. J. Zhang, and C. C. Wong, "Laser directed deposition of silver thin films," *Thin Solid Films*, vol. 519, no. 15, pp. 5183–5187, 2011.

[22] L. Mini, C. Giaconia, and C. Arnone, "Copper patterning on dielectrics by laser writing in liquid solution," *Applied Physics Letters*, vol. 64, no. 25, pp. 3404–3406, 1994.

[23] K. Kordás, "Laser direct writing of copper on polyimide surfaces from solution," *Applied Surface Science*, vol. 154-155, no. 1-4, pp. 399–404, 2000.

[24] A. Manshina, A. Povolotskiy, T. Ivanova, A. Kurochkin, Y. Tver'yanovich, D. Kim, M. Kim, and S. C. Kwon, "Cucl2-based liquid electrolyte precursor for laser-induced metal deposition," *Laser Physics Letters*, vol. 4, no. 3, pp. 242–246, 2007.

[25] A. Ouchi, Z. Bastl, J. Boháček, J. Šubrt, and J. Pola, "Laser-induced chemical liquid deposition of discontinuous and continuous copper films," *Surface and Coatings Technology*, vol. 201, no. 8, pp. 4728–4733, 2007.

[26] M.-S. Li and C.-X. Yang, "Laser-induced silver nanoparticles deposited on optical fiber core for surface-enhanced raman scattering," *Chinese Physics Letters*, vol. 27, no. 4, p. 044202, 2010.

[27] Y. Niidome, A. Hori, H. Takahashi, Y. Goto, and S. Yamada, "Laser-induced deposition of gold nanoparticles onto glass substrates in cyclohexane," *Nano Letters*, vol. 1, no. 7, pp. 365–369, 2001.

[28] G. Toth, K. Kordas, J. Vahakangas, A. Uusimaki, T. F. George, and L. Nanai, "Laser-induced gold deposition on p(+)-si from liquid precursors: A study on the reduction of gold ions through competing dember and seebeck effects," *Journal of Physical Chemistry B*, vol. 109, no. 15, pp. 6925–6928, 2005.

[29] M. Brust, M. Walker, D. Bethell, D. J. Schiffrin, and R. Whyman, "Synthesis of thiol-derivatised gold nanoparticles in a two-phase liquid-liquid system," *Journal of the Chemical Society, Chemical Communications*, no. 7, p. 801, 1994.

[30] J. P. Blondeau and O. Veron, "Precipitation of silver nanoparticles in glass by multiple wavelength nanosecond laser irradiation," *Journal of optoelectronics and advanced materials*, vol. 12, no. 3, pp. 445–450, 2010.

[31] E. J. Bjerneld, K. V. G. K. Murty, J. Prikulis, and M. Käll, "Laser-induced growth of ag nanoparticles from aqueous solutions," *ChemPhysChem*, vol. 3, no. 1, pp. 116–119, 2002.

[32] H. Hidaka, H. Honjo, S. Horikoshi, and N. Serpone, "Photoinduced agn0 cluster deposition: Photoreduction of ag+ ions on a tio2-coated quartz crystal microbalance monitored in real time," *Sensors and Actuators B: Chemical*, vol. 123, no. 2, pp. 822–828, 2007.

[33] J. C. Vinci, P. Bilski, R. Kotek, and C. Chignell, "Controlling the formation of silver nanoparticles on silica by photochemical deposition and other means," *Photochemistry and Photobiology*, vol. 86, no. 4, pp. 806–812, 2010.

[34] A. A. Tseng, A. Notargiacomo, and T. P. Chen, "Nanofabrication by scanning probe microscope lithography: A review," *Journal of Vacuum Science & Technology B*, vol. 23, no. 3, pp. 877–894, 2005.

[35] X. N. Xie, H. J. Chung, C. H. Sow, and A. T. S. Wee, "Nanoscale materials patterning and engineering by atomic force microscopy nanolithography," *Materials Science & Engineering R-Reports*, vol. 54, no. 1-2, pp. 1–48, 2006.

[36] L. G. Rosa and J. Liang, "Atomic force microscope nanolithography: dip-pen, nanoshaving, nanografting, tapping mode, electrochemical and thermal nanolithography," *J Phys Condens Matter*, vol. 21, no. 48, p. 483001, 2009.

[37] A. A. Tseng, "Three-dimensional patterning of nanostructures using atomic force microscopes," *Journal of Vacuum Science and Technology B: Microelectronics and Nanometer Structures*, vol. 29, no. 4, pp. 040801–21, 2011.

[38] M. Yasutake, Y. Ejiri, and T. Hattori, "Modification of silicon surface using atomic-force microscope with conducting probe," *Japanese Journal of Applied Physics Part 2-Letters*, vol. 32, no. 7B, pp. L1021–L1023, 1993.

[39] J. A. Dataga, "Device fabrication by scanned probe oxidation," *Science*, vol. 270, no. 5242, pp. 1625–1626, 1995.

[40] M. A. McCord and R. F. W. Pease, "Lift-off metallization using poly(methylmethacrylate) exposed with a scanning tunneling microscope," *Journal of Vacuum Science & Technology B*, vol. 6, no. 1, pp. 293–296, 1988.

[41] W. K. Lee, S. Chen, A. Chilkoti, and S. Zauscher, "Fabrication of gold nanowires by electric-field-induced scanning probe lithography and in situ chemical development," *Small*, vol. 3, no. 2, pp. 249–54, 2007.

[42] R. C. Barrett and C. F. Quate, "Charge storage in a nitrideoxidesilicon medium by scanning capacitance microscopy," *Journal of Applied Physics*, vol. 70, no. 5, pp. 2725–2733, 1991.

[43] R. Crook, A. C. Graham, C. G. Smith, I. Farrer, H. E. Beere, and D. A. Ritchie, "Erasable electrostatic lithography for quantum components," *Nature*, vol. 424, no. 6950, pp. 751–4, 2003.

[44] S. Xu and G. Y. Liu, "Nanometer-scale fabrication by simultaneous nanoshaving and molecular self-assembly," *Langmuir*, vol. 13, no. 2, pp. 127–129, 1997.

[45] S. Kramer, R. R. Fuierer, and C. B. Gorman, "Scanning probe lithography using self-assembled monolayers," *Chemical Reviews*, vol. 103, no. 11, pp. 4367–4418, 2003.

[46] R. Magno and B. R. Bennett, "Nanostructure patterns written in iii-v semicondcutors by an atomic force microscope," *Applied Physics Letters*, vol. 70, no. 14, pp. 1855–1857, 1997.

[47] H. Takano and M. Fujihira, "Afm microlithography of a thin chromium film covered with a thin resist langmuir-blodgett (lb) film," *Thin Solid Films*, vol. 273, no. 1-2, pp. 312–316, 1996.

[48] D. Saulys, G. Rudd, and E. Garfunkel, "Scanning tunneling microscopy assisted oxide surface etching," *Journal of Applied Physics*, vol. 69, no. 3, p. 1707, 1991.

[49] N. Li, T. Yoshinobu, and H. Iwasaki, "Low energy electron beam stimulated surface reaction: Selective etching of sio2/si using scanning tunneling microscope," *Japanese Journal of Applied Physics Part 2-Letters*, vol. 37, no. 8B, pp. L995–L998, 1998.

[50] L. A. Nagahara, T. Thundat, and S. M. Lindsay, "Nanolithography on semiconductor surfaces under an etching solution," *Applied Physics Letters*, vol. 57, no. 3, p. 270, 1990.

[51] R. E. Thomson, J. Moreland, and A. Roshko, "Surface modification of yba2cu3o7-d thin films using the scanning tunneling microscope-five methods," *Nanotechnology*, vol. 5, pp. 57–69, 1994.

[52] C. Kaneshiro and T. Okumura, "Nanoscale etching of gaas surfaces in electrolytic solutions by hole injection from a scanning tunneling microscope tip," *Journal of Vacuum Science & Technology B*, vol. 15, no. 5, pp. 1595–1598, 1997.

[53] H. J. Mamin, "Thermal writing using a heated atomic force microscope tip," *Applied Physics Letters*, vol. 69, no. 3, pp. 433–435, 1996.

[54] P. Vettiger, G. Cross, M. Despont, U. Drechsler, U. Durig, B. Gotsmann, W. Haberle, M. A. Lantz, H. E. Rothuizen, R. Stutz, and G. K. Binnig, "The "millipede" - nanotechnology entering data storage," *Nanotechnology, IEEE Transactions on*, vol. 1, no. 1, pp. 39–55, 2002.

[55] H. Mamin, P. Guethner, and D. Rugar, "Atomic emission from a gold scanning-tunneling-microscope tip," *Physical Review Letters*, vol. 65, no. 19, pp. 2418–2421, 1990.

[56] S. Hosaka, H. Koyanagi, and A. Kikukawa, "Nanometer recording on graphite and si substrate using an atomic force microscope in air," *Japanese Journal of Applied Physics Part 2-Letters*, vol. 32, no. 3B, pp. L464–L467, 1993.

[57] D. Fujita, K. Onishi, and T. Kumakura, "Silver nanostructures formation on si(111)-(7x7) surfaces by the tip of a scanning tunneling microscope," *Japanese Journal of Applied Physics*, vol. 42, no. Part 1, No. 7B, pp. 4773–4776, 2003.

[58] R. M. Silver, E. E. Ehrichs, and A. L. de Lozanne, "Direct writing of submicron metallic features with a scanning tunneling microscope," *Applied Physics Letters*, vol. 51, no. 4, p. 247, 1987.

[59] W. W. Pai, J. Zhang, and J. F. Wendelken, "Magnetic nanostructures fabricated by scanning tunneling microscope-assisted chemical vappor deposition," *Journal of Vacuum Science & Technology B*, vol. 15, no. 4, pp. 785–787, 1997.

[60] W. Schindler, D. Hofmann, and J. Kirschner, "Nanoscale electrodeposition: A new route to magnetic nanostructures?," *Journal of Applied Physics*, vol. 87, no. 9, p. 7007, 2000.

[61] D. S. Ginger, H. Zhang, and C. A. Mirkin, "The evolution of dip-pen nanolithography," *Angew Chem Int Ed Engl*, vol. 43, no. 1, pp. 30–45, 2004.

[62] Y. Li, B. W. Maynor, and J. Liu, "Electrochemical afm "dip-pen" nanolithography," *J Am Chem Soc*, vol. 123, no. 9, pp. 2105–6, 2001.

[63] P. T. Hurley, A. E. Ribbe, and J. M. Buriak, "Nanopatterning of alkynes on hydrogen-terminated silicon surfaces by scanning probe-induced cathodic electrografting," *J Am Chem Soc*, vol. 125, no. 37, pp. 11334–9, 2003.

[64] M. Sitti and H. Hashimoto, "Controlled pushing of nanoparticles: Modeling and experiments," *Ieee-Asme Transactions on Mechatronics*, vol. 5, no. 2, pp. 199–211, 2000.

[65] C. Ritter, M. Heyde, U. D. Schwarz, and K. Rademann, "Controlled traslational manipulation of small latex spheres by dynamic force microscopy," *Langmuir*, vol. 18, pp. 7798–7803, 2002.

[66] M. Heyde, B. Cappella, H. Sturm, C. Ritter, and K. Rademann, "Dislocation of antimony clusters on graphite by means of dynamic plowing nanolithography," *Surface Science*, vol. 476, no. 1-2, pp. 54–62, 2001.

[67] D. M. Schaefer, R. Reifenberger, A. Patil, and R. P. Andres, "Fabrication of two-dimensional arrays of nanometer-size clusters with the atomic force microscope," *Applied Physics Letters*, vol. 66, no. 8, p. 1012, 1995.

[68] J. K. Gimzewski and C. Joachim, "Nanoscale science of single molecules using local probes," *Science*, vol. 283, no. 5408, pp. 1683–1688, 1999.

[69] D. M. Eigler and E. K. Schweizer, "Positioning single atoms with a scanning tunneling microscope," *Nature*, vol. 344, no. 6266, pp. 524–526, 1990.

[70] S.-W. Hla, K.-F. Braun, and K.-H. Rieder, "Single-atom manipulation mechanisms during a quantum corral construction," *Physical Review B*, vol. 67, no. 20, 2003.

[71] J. A. Strocio and R. J. Celotta, "Controlling the dynamics of a single atom in lateral atom manipulation," *Science*, vol. 306, no. 5694, pp. 242–247, 2004.

[72] J. Hu, Y. Zhang, H. Gao, M. Li, and U. Hartmann, "Artificial dna patterns by mechanical nanopanipulation," *Nano Letters*, vol. 2, no. 1, pp. 55–57, 2002.

[73] J. H. Lu, H. K. Li, H. J. An, G. H. Wang, Y. Wang, M. Q. Li, Y. Zhang, and J. Hu, "Positioning isolation and biochemical analysis of single dna molecules based on nanomanipulation and single-molecule pcr," *J Am Chem Soc*, vol. 126, no. 36, pp. 11136–7, 2004.

[74] P. E. Sheehan and C. M. Lieber, "Nanotribology and nanofabrication of moo3 structures by atomic force microscopy," *Science*, vol. 272, no. 5265, pp. 1158–61, 1996.

[75] I. W. Lyo and P. Avouris, "Field-induced nanometer- to atomic-scale manipulation of silicon surfaces with the stm," *Science*, vol. 253, no. 5016, pp. 173–6, 1991.

[76] C. T. Salling and M. G. Lagally, "Fabrication of atomic-scale structures on si(001) surfaces," *Science*, vol. 265, no. 5171, pp. 502–6, 1994.

[77] S. C. Hsieh, S. Meltzer, C. R. C. Wang, A. A. G. Requicha, M. E. Thompson, and B. E. Koel, "Imaging and manipulation of gold nanorods with an atomic force microscope," *Journal of Physical Chemistry B*, vol. 106, no. 2, pp. 231–234, 2002.

[78] L. Roschier, J. Penttilä, M. Martin, P. Hakonen, M. Paalanen, U. Tapper, E. I. Kauppinen, C. Journet, and P. Bernier, "Single-electron transistor made of multiwalled carbon nanotube using scanning probe manipulation," *Applied Physics Letters*, vol. 75, no. 5, p. 728, 1999.

[79] H. Xie, D. S. Haliyo, and S. Regnier, "A versatile atomic force microscope for three-dimensional nanomanipulation and nanoassembly," *Nanotechnology*, vol. 20, no. 21, p. 215301, 2009.

[80] Z. H. Mai, Y. F. Lu, W. D. Song, and W. K. Chim, "Nano-modification on hydrogen-passivated si surfaces by a laser-assisted scanning tunneling microscope operating in air," *Applied Surface Science*, vol. 154, pp. 360–364, 2000.

[81] Y. F. Lu, B. Hu, Z. H. Mai, W. J. Wang, W. K. Chim, and T. C. Chong, "Laser-scanning probe microscope based nanoprocessing of electronics materials," *Japanese Journal of Applied Physics Part 1-Regular Papers Short Notes & Review Papers*, vol. 40, no. 6B, pp. 4395–4398, 2001.

[82] A. Chimmalgi, T. Y. Choi, C. P. Grigoropoulos, and K. Komvopoulos, "Femtosecond laser aperturless near-field nanomachining of metals assisted by scanning probe microscopy," *Applied Physics Letters*, vol. 82, no. 8, p. 1146, 2003.

[83] X. Yin, N. Fang, X. Zhang, I. B. Martini, and B. J. Schwartz, "Near-field two-photon nanolithography using an apertureless optical probe," *Applied Physics Letters*, vol. 81, no. 19, p. 3663, 2002.

[84] K. J. Yi, Z. Y. Yang, and Y. F. Lu, "Fabrication of nanostructures with high electrical conductivity on silicon surfaces using a laser-assisted scanning tunneling microscope," *Journal of Applied Physics*, vol. 103, no. 5, p. 054307, 2008.

[85] D. Haefliger and A. Stemmer, "Writing subwavelength-sized structures into aluminium films by thermo-chemical aperture-less near-field optical microscopy," *Ultramicroscopy*, vol. 100, no. 3-4, pp. 457–64, 2004.

[86] A. A. Tseng, "Recent developments in nanofabrication using scanning near-field optical microscope lithography," *Optics & Laser Technology*, vol. 39, no. 3, pp. 514–526, 2007.

[87] M. Harada and H. Einaga, "In situ xafs studies of au particle formation by photoreduction in polymer solutions," *Langmuir*, vol. 23, no. 12, pp. 6536–43, 2007.

[88] E. J. Bjerneld, F. Svedberg, and M. Käll, "Laser-induced growth and deposition of noble-metal nanoparticles for surface-enhanced raman scattering," *Nano Letters*, vol. 3, no. 5, pp. 593–596, 2003.

[89] B. Novotny, Lukas; Hecht, *Principle of nano-optics*. Cambridge University Press, 2006.

[90] L. Jian-Hui, H. Lan, and G. Ning, "Fabrication of nanoparticle pattern through atomic force microscopy tip-induced deposition on modified silicon surfaces," *Chinese Physics Letters*, vol. 19, no. 1, pp. 134–136, 2002.

[91] R. H. French and H. V. Tran, "Immersion lithography: Photomask and wafer-level materials," *Annual Review of Materials Research*, vol. 39, pp. 93–126, 2009.

[92] T. P. Inc., "Toppan photomasks, inc. - euv masks - the world's premier photomask company." http://www.photomask.com/products/euv-masks, 2012.

VITA

Carlos Andrés Jarro Sanabria was born on May 10, 1976 in Cali, Colombia. He received his B.S. degree from the Department of Electronic Engineering at Pontifical University Xaveriana in Bogotá, Colombia, in November 2001. He acquired practical experience while working as a control engineer in Bogotá and then as a supervisory control and data acquisition maintenance engineer in Caño Limón. In 2008 he went back to school to pursue a PhD degree in Electrical Engineering and entered in the University of Kentucky in Lexington. He is working now under the direction of Dr. Todd Hastings on his nanotechnology research group.

Publications:

- P.A. Liu, V.P. Singh, C.A. Jarro, S. Rajaputra, "Cadmium sulfide nanowires for the window semiconductor layer in thin film CdS-CdTe solar cells," Nanotechnology, vol. 22, no. 14, pp.9 ,2011.